



Cite this: *Chem. Soc. Rev.*, 2017,  
**46**, 5588

Received 13th October 2016

DOI: 10.1039/c6cs00738d

rsc.li/chem-soc-rev

## Materials learning from life: concepts for active, adaptive and autonomous molecular systems

Rémi Merindol and Andreas Walther\*

Bioinspired out-of-equilibrium systems will set the scene for the next generation of molecular materials with active, adaptive, autonomous, emergent and intelligent behavior. Indeed life provides the best demonstrations of complex and functional out-of-equilibrium systems: cells keep track of time, communicate, move, adapt, evolve and replicate continuously. Stirred by the understanding of biological principles, artificial out-of-equilibrium systems are emerging in many fields of soft matter science. Here we put in perspective the molecular mechanisms driving biological functions with the ones driving synthetic molecular systems. Focusing on principles that enable new levels of functionalities (temporal control, autonomous structures, motion and work generation, information processing) rather than on specific material classes, we outline key cross-disciplinary concepts that emerge in this challenging field. Ultimately, the goal is to inspire and support new generations of autonomous and adaptive molecular devices fueled by self-regulating chemistry.

Institute for Macromolecular Chemistry, Albert-Ludwigs-University Freiburg,  
 Stefan-Meier Strasse 31, 79106 Freiburg, Germany.  
 E-mail: [andreas.walther@makro.uni-freiburg.de](mailto:andreas.walther@makro.uni-freiburg.de)



Rémi Merindol

Dr Rémi Merindol received his PhD from the University of Strasbourg in 2014. There he explored the layer-by-layer assembly and mechanical characterization of wood- and nacre-inspired materials in the group of Prof. Gero Decher. Currently he carries out postdoctoral research in the team of Prof. Andreas Walther at the Albert-Ludwigs-University of Freiburg. Inspired by living soft materials, his research interests focus on new non-equilibrium

materials with a molecularly precise architecture and time-controlled dynamics.

### 1. Introduction

A fruit fly lands on an apple, another event mesmerizing in complexity goes unnoticed. The millimeter big fly consists of a



Andreas Walther

Prof. Dr Andreas Walther is a Professor for Functional Polymers at the Institute for Macromolecular Chemistry at the Albert-Ludwigs-University in Freiburg (Germany). His research interests concentrate on developing and understanding hierarchical self-assembly concepts inside and outside equilibrium, and on using them to create active, adaptive and autonomous bioinspired material systems. He graduated from Bayreuth University in Germany in 2008

with a PhD focusing on the self-assembly behavior and applications of Janus particles and other soft, complex colloids. After a postdoctoral stay with a focus on biomimetic hybrid materials at Aalto University (Helsinki, Finland), he returned to Germany (2011), and established his independent research group at the DWI – Leibniz Institute for Interactive Materials in Aachen. In 2016 he was appointed to his present position in Freiburg. A. Walther has published close to 120 papers (*h*-index 42) and has recently been awarded the Bayer Early Excellence in Science Award (for Materials), the Reimund Stadler Young Investigator Award of the German Chemical Society, a BMBF NanoMatFutur Research Group, and an ERC Starting Grant.

dissipative, self-organized molecular system fueled by glucose oxidation, and capable of autonomous flight, sensing and adaptation for hours. Such complex chemical out-of-equilibrium systems are ubiquitous in living organisms. In fact, most life-distinguishing features rely on non-equilibrium dynamics, involving constant energy dissipation, kinetic control, and are orchestrated through feedback loops.

We are now at a point in time, where an increasing amount of molecular mechanisms at the origin of these functions in living organisms has been unraveled. They provide a considerable source of inspiration for new generations of molecular materials and systems with unprecedented levels of functionalities – adaptive and interactive properties. Temporal control, the ability to accumulate work, sensing, adaptation or communication depend on dissipative chemical systems, and the ultimate goal of life-like, self-organizing systems requires to combine and integrate them using feedback loops.

In contrast, synthetic chemistry, soft matter nanoscience and materials research have mostly focused on the generation of equilibrium or metastable (kinetically trapped) structures. Progress in the synthesis of intrinsically functional building blocks (*e.g.* conducting polymers), hybridization with (in)organic nanomaterials or biological moieties has greatly contributed to reach a high level of structural control through molecular design (space domain), and to integrate functional properties.

Such materials have become switchable *via* responsive molecular components. Yet the switching of states always requires an outside trigger and autonomous behavior is largely absent (aside simple relaxation events).

The next disruptive change in the property profiles of soft matter will arise from developing far-from-equilibrium, fueled and feedback-controlled molecular systems, because they can show orchestrated, pre-programmed and autonomous dynamics in the time domain, because they will be able to sense, adapt, communicate, learn, evolve and replicate, and because it will take the present-day “dead” materials to a more interactive, intelligent and life-like state (Fig. 1). Even though this is a profound challenge and in parts a distant dream for soft matter research, the understanding of molecular biological mechanisms and the

design of synthetic out-of-equilibrium molecular systems are improving quickly, and it is timely to identify some unifying and thought-provoking principles.

In this review, we aim to fuel the inspiration of scientists with examples from biology, and steer cross-disciplinary exchange of knowledge and concepts towards new functional autonomous molecular devices and material systems.

We focus on functions and their underlying enabling principles rather than on a specific field of chemistry or soft matter nanoscience. We identify four categories of functions that rely upon out-of-equilibrium systems:

- temporal control (Section 2)
- autonomous structures (Section 3)
- motion and mechanical work (Section 4)
- information processing (Section 5)

We will use biological mechanisms at the origin of these functions to illustrate each category and point to some ultimate goals. Without aiming to be exhaustive, we discuss the most relevant publications across the fields of non-linear, enzymatic, supramolecular and DNA-based chemistries. Some outlooks from computer simulations are also reviewed.

Our goal is to outline some strong and weak points of different types of chemistries to achieve a given function – indeed future outcomes are hardly predictable.<sup>1</sup> Whenever appropriate we direct the reader to specific reviews related to relevant topics. We recommend complementary perspectives on supramolecular systems chemistry,<sup>2</sup> reaction/diffusion in nanotechnology,<sup>3</sup> temporal programming of self assemblies,<sup>4</sup> programmable reaction networks,<sup>5</sup> non-equilibrium nanomaterials,<sup>6</sup> the physics of pattern formation,<sup>7</sup> or life's relation to nanotechnology<sup>8</sup> and supramolecular assemblies.<sup>9</sup>

We are confident that this cross-disciplinary review will stimulate further research in the exciting new area of out-of-equilibrium molecular systems engineering – where autonomous functions and intelligent materials can be designed.

## 2. Temporal regulation of chemical potentials

In this section we introduce the mechanisms at the origin of temporal regulation in biological and synthetic systems. We review how oscillating reactions, initially disregarded, can now be rationally engineered in synthetic molecular systems. At this point we mostly focus on the temporal regulation of chemical potentials and chemical species. Later on, we will connect these tools to autonomous structure formation, work generation and information processing.

### 2.1. Temporal control in biological systems

Living organisms present a multitude of synchronized or disconnected time-regulated functions. Cells periodically alternate growth and division, the heart pumps blood with rhythmic pacemaker activity, and the metabolism of most living organisms is synchronized with the night and day cycle on earth. These oscillations are controlled by chemical signals forming a

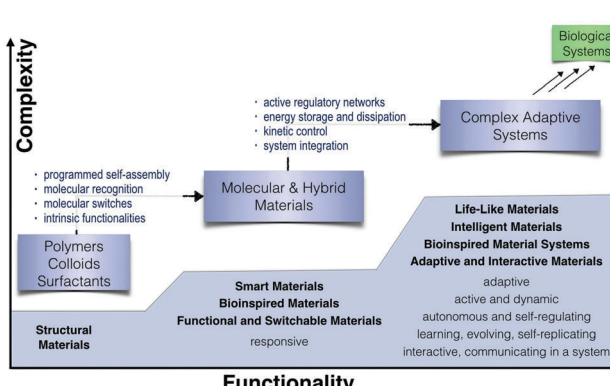


Fig. 1 Correlation between complexity and functionality in molecular systems. From structural control to responsive and adaptive systems.

hierarchical regulatory network consisting of independent sub-unit oscillators with different characteristic time scales that communicate with each other.

Provided that the molecular signals are degraded at a constant rate, oscillatory behavior only requires a feedback control of their formation rate. An oscillatory mechanism requires at least a negative feedback loop, which allows the system to return to its starting point. The negative feedback reduces the production rate of a molecular signal when its quantity in the system increases, prompting the signal level to return to its original value as the constant degradation takes over. In Fig. 2A this corresponds to an increase of the negative regulator “b” when the quantity of “a” increases (see Fig. 2A–C for the basic formalism of regulatory networks). The negative feedback loop must be delayed in time to prevent stabilization of an intermediate steady state (where formation and degradation balance each other; an example of a delayed negative feedback is given in Fig. 2B). Although these conditions are sufficient to obtain chemical oscillations, most biological systems also include a positive feedback mechanism (Fig. 2C) to further increase the robustness of the oscillations (also Fig. 2F).<sup>10,11</sup>

For instance, the circadian clock is an oscillating system with a period of 24 hours that synchronizes physiological functions such as sleep cycles, glucose metabolism and cell-replication with the day and night cycles on earth. This oscillator relies on several transcription-translation-regulation feedback loops (Fig. 2D–F). In mammals, a protein complex, CLOCK-BMAL1, binds to the nucleic DNA and activates the transcription of a gene coding for their own inhibitors, the PER and CRY proteins (negative feedback). These proteins accumulate in the cytoplasm after translation, undergo post-translational phosphorylation (time delay enabling 24 hours long oscillation period) and eventually re-enter the nucleus to repress their activation by the CLOCK-BMAL1 complex. This reduces the transcription of the PER gene leading to a decrease of PER proteins, and hence allowing for a new cycle to start.<sup>12,13</sup> In parallel the CLOCK-BMAL1 complex activates the expression of ROR and REV-ERB genes that respectively activate (positive feedback) and repress the expression of BMAL1 stabilizing the oscillatory behavior.<sup>14</sup> This 24 hour core oscillator then couples to peripheral oscillators to guide further macroscopic functions (Fig. 2D).<sup>15</sup>

This robust feedback system allows the core and the peripheral oscillators to maintain their periods for days even when extracted from the organism (Fig. 2E).<sup>16,17</sup> The overall behavior demonstrates processes that are coupled hierarchically in the time domain – an important principle.

At the other extreme, the fast oscillations of the trans-membrane potentials in nerves actuate muscle contractions, and maintain the cardiac pacemaker activity with a period of seconds. The propagation of a single oscillation of the trans-membrane potential consists of the cooperative opening (positive feedback) of sodium and potassium channels upon depolarization allowing fast propagation of the electric signal, while slower ATP-fueled sodium-potassium pumps regenerate

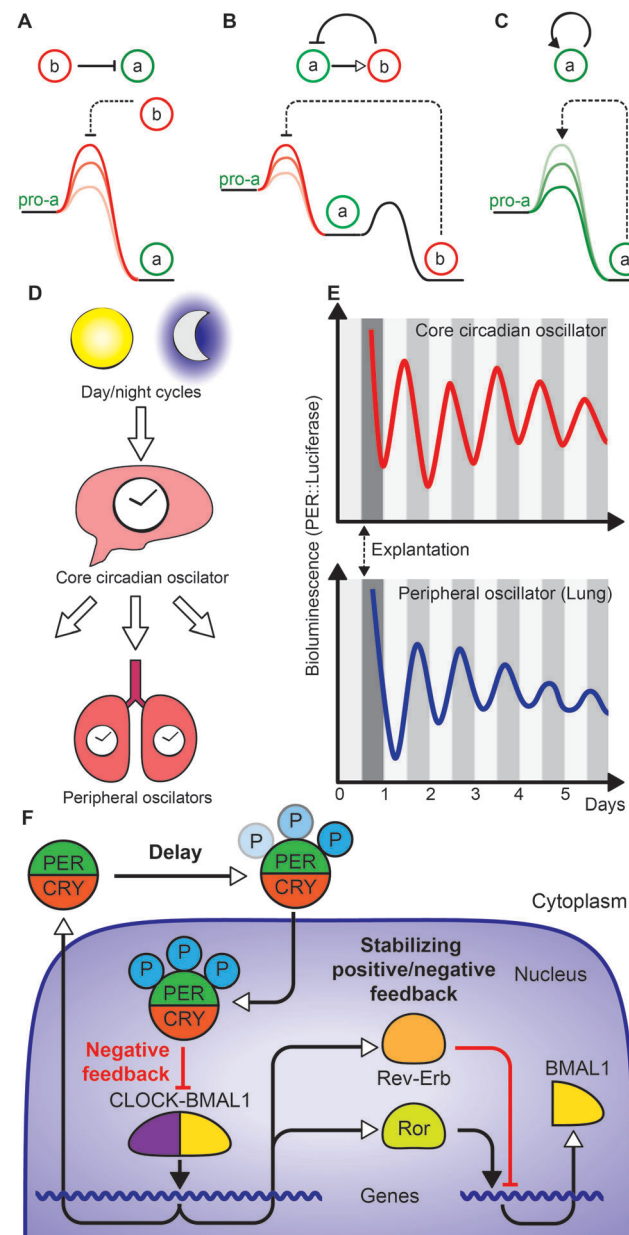


**Fig. 2** Biological regulatory networks for autonomous temporal control. (A) Schematic representation of the down-regulation of “a” production by “b”, symbolized by an arrow with a flat head (top), and an exemplarily corresponding reaction profile, where the amount of signal “b” is positively correlated with the activation barrier of formation of “a” (bottom). (B) Schematic representation and reaction rate profile of a delayed negative feedback, where the delay induced by the transformation of “a” into “b” is represented by an arrow with empty head. (C) Autocatalytic positive feedback for the formation of “a”, symbolized by an arrow with a filled head (top), and the corresponding reaction profile, where “a” decreases its own activation barrier of formation (bottom). (D) Schematic representation of the hierarchical circadian network, in which the core clock synchronizes the metabolic clock in the lungs while being regulated by the day/night cycles. (E) Real time visualization of PER expression using PER::luciferase fusion proteins in the supercharismatic nucleus (core oscillators) and in lungs (peripheral oscillators) in mice. Tissues were explanted at day 0.5, white and dark lines show day/night cycles. (F) Schematic representation of the feedback loops controlling circadian oscillations. Adapted with permission from (E) ref. 16 Copyright 2004, the National Academy of Sciences and (F) ref. 13 Copyright 2007, Nature Publishing Group.

the trans-membrane potential after signal propagation (delay).<sup>18,19</sup> Hyperpolarization-activated ion channels provide the negative feedback mechanism necessary to drive autonomous oscillation. These channels open at high cross-membrane potential and spontaneously trigger new action potentials by depolarizing the membrane below the propagation threshold to generate an autonomous pacemaker activity. Their activation voltage, regulated by the presence of cyclic nucleotides (cAMP), is adjusted in the function of the oxygen demand of the organism and controls the heartbeat rate.<sup>20</sup>

Overall, temporal control in living organisms relies on combinations of positive and negative feedback loops, as well as delay mechanisms. The diverse molecular effectors of these mechanisms (cross membrane potential, gene expression or enzyme activity...) define the characteristic time scales of the systems. Engineering time delays is crucial. Many of these systems also interact and synchronize with each other in a hierarchical fashion (for example the slow circadian cycle regulates the fast pacemaker activity). Finally, in addition to autonomous temporal control, these networks involve further adaptation mechanisms that adjust the temporal control to variations of external parameters (jet-lag, effort induced tachycardia...), making them adaptive to external signals.

Although feedback-regulated reactions are common in biological organisms, their implementation in synthetic systems is challenging, in particular for autonomous systems.

## 2.2. Synthetic oscillators in open and closed reactors

The fascination for non-linear, feedback-controlled chemical reactions emerged with the discovery of an oscillating reaction by Belousov in the early 50s,<sup>21</sup> later developed and brought to broader attention by Zhabotinsky.<sup>22</sup> The system consists of a solution of sulfuric acid, potassium bromate, malonic acid and a catalytic amount of cerium sulfate to produce brominated malonic acid as well as formic acid. Sustained oscillations of the concentrations of bromide and cerium(IV) form during this transformation based on a complex chemical reaction network, whose exact mechanism involves more than 10 individual reactions.<sup>23</sup> The core of the oscillating process relies on the autocatalytic formation of bromous acid ( $\text{HBrO}_2$ ) (positive feedback) that is inhibited by the later formation of bromine (delayed negative feedback). Cerium ions are oxidized and reduced stoichiometrically during each cycle, leading to periodic color variations. The catalytic amount of cerium limits the autocatalytic formation of the bromous acid intermediate and maintains oscillations in closed reactors (Fig. 3A and C).

Other synthetic chemical oscillators in a closed system are scarce.<sup>24,25</sup> One of the reasons is that, in addition to non-linear chemical reactions regulated by suitable positive and negative feedback, sustained oscillations require a constant formation and degradation of the interacting chemicals, which is profoundly challenging to *de novo* engineer in a closed and homogeneous system.

One way to explore new oscillating reactions is to use open reactors (Continuous Stirred Tank Reactors, CSTRs), where the

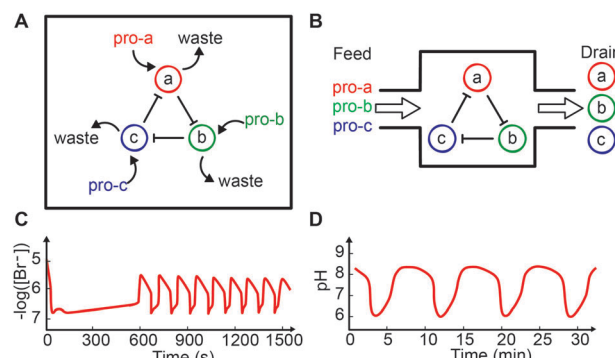


**Fig. 3** Oscillations of chemical potential from synthetic feedback-regulated systems. The minimal reaction system generating sustained oscillations (for a triple negative feedback loop) (A) in a closed reactor and (B) in an open continuous flow stirred tank reactor (CSTR). (C) Example of the spontaneous bromide oscillation in the Belousov–Zhabotinsky (BZ) reaction in a closed system. (D) Example of a pH oscillation in an open CSTR based on the sulphide/hydrogen peroxide reaction. Adapted with permission from (C) ref. 23 Copyright 1972, the American Chemical Society, and (D) ref. 35 Copyright 1985, the American Chemical Society.

reactants can be fed and the products drained (Fig. 3B).<sup>26</sup> The use of such open reactors has led to the development of dozens of new synthetic oscillating reactions.<sup>27–32</sup> Among those, pH-oscillators are especially interesting because pH is one of the most ubiquitous stimuli for the actuation of soft responsive materials (Fig. 3D).<sup>33–37</sup> While the development of oscillations in open reactors helps to understand non-equilibrium chemical dynamics, their possible applications in functional systems may be limited – in particular regarding the level of autonomy. Tricks to overcome constant feeding and drainage involve compartmentalization. For example the key reactants of an oscillating reaction can be loaded in a silica bed from which they slowly diffuse back in solution, leading to the equivalent of a semi-batch reactor. As the reactants are constantly fed (from the silica to the solution), such a design enables the generation of sustained pH oscillations in a closed system.<sup>38</sup>

Even though there has been progress in the direction of other oscillators, the Belousov–Zhabotinsky (BZ) reaction remains one of the main workhorses for the exploration of functional out-of-equilibrium oscillating systems. This is due to the long lasting periodic oscillations, the possibility to tune the kinetics by light,<sup>39</sup> or chemicals,<sup>40</sup> as well as the easy coupling with redox responsive materials.<sup>41</sup>

Overall, most inorganic feedback-controlled systems, including the BZ reaction, rely on comparably harsh and toxic reactants such as concentrated acids, halogen derivatives and transition metals, which limits their developments beyond the proof of concept stage. Hence, the design of feedback-controlled reactions under mild conditions is of prime interest for the development of user-friendly, environmentally benign and potentially even biocompatible functional devices. For instance, a system based on the competing base-catalyzed hydrolysis of gluconolactone (lowering the pH) and formaldehyde-sulfite reactions (increasing the pH) in a constantly fed

reaction led to pH oscillations without halogen or transition metal derivatives (yet the presence of formaldehyde remains problematic).<sup>42</sup>

### 2.3. Biocatalytic temporal control under mild conditions

An interesting alternative for the design of benign oscillators consists in the development of hybrid systems combining synthetic chemicals and enzymatic reactions. Cascades of enzymatic reactions are at the origin of many temporal regulation mechanisms in living organisms. While this has been known for a long time,<sup>43</sup> the translation into the synthetic world has been limited by the availability of purified enzymes and complex experimental setups.<sup>44–46</sup>

Recently, research in this direction has however been blossoming. Focusing first on pH-modulating systems, it was for instance shown that the glucose oxidase-catalyzed hydrolysis of glucose in the presence of ferricyanide generates a time-controlled pH-drop in a closed system. Oscillations could also be forced using a computer-assisted negative feedback.<sup>47</sup> An opposite time-controlled pH-jump in a closed system was demonstrated based on the enzymatic urea/urease system. The reaction also displays bistability and oscillatory behavior in open CSTRs.<sup>48</sup>

The origin of the temporal control in these systems relies on the pH-dependent activity of enzymes that self-regulates (feedback) by acid or base production (Fig. 4A). For instance, urease is more active at pH 7 than at pH 3. When urea is mixed with urease at pH 3.5, the initial activity of the urease is low and urea is slowly hydrolyzed into ammonia. As ammonia accumulates in the mixture, the pH progressively increases, thereby increasing the production rate of ammonia and eventually leading to the abrupt transition from low to high pH at the maximum of urease activity (Fig. 4A and B).

A further exciting example of the great potential of enzymatic reaction networks for the design of temporal control mechanisms under mild conditions relies on the autocatalytic conversion of trypsinogen to trypsin.<sup>50</sup> Trypsin (Tr) is a protease capable of hydrolyzing a peptide chain next to a lysine or arginine residue. Trypsinogen (Tg) is a trypsin precursor inactivated by the presence of a lysine bound tail. Trypsin can therefore catalyze its own formation from trypsinogen (hydrolysis at the lysine residue), naturally leading to a positive feedback. A trypsin-inhibitor precursor that is activated by trypsin (similar mechanism) generates a negative feedback loop. The addition of a supplementary enzyme-controlled deprotection step before the trypsin inhibitor becomes active implements the delay necessary to obtain oscillations (Fig. 4C–E). The system displays oscillations in open reactors (CSTR) and the periods can be adjusted between 5 and 10 hours depending on the flow rate and composition of the feed solutions. Another beneficial feature of bio-catalytic systems is their sensitivity to the molecular structure of the interacting species. Hence, small changes in the protecting group of the trypsin-inhibitor dramatically modify the behavior of the oscillatory reaction.<sup>51</sup>

Obviously, the increasing understanding of enzyme kinetics and the broader availability of purified and re-engineered enzymes open up new opportunities to design biocatalytic systems for

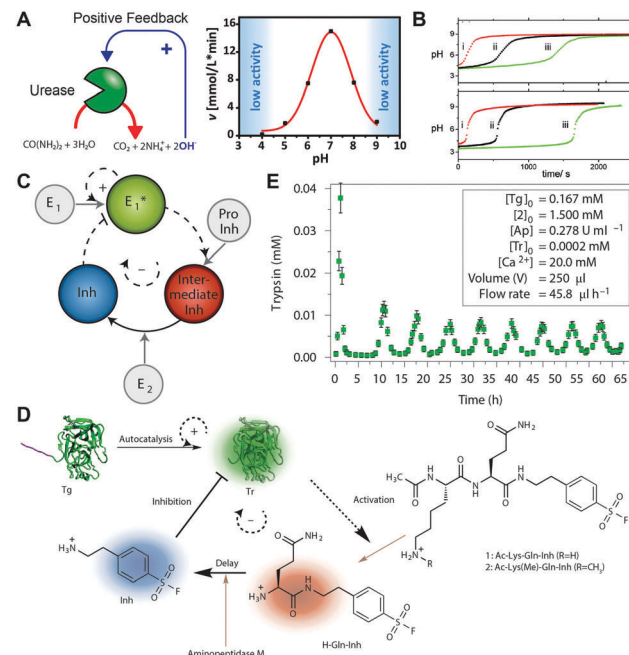


**Fig. 4** Enzymatic systems for temporal regulation. (A) Schematic representation of positive feedback for urea/urease system under acidic conditions together with the bell-shaped activity curve of urease. (B) pH profile of a system containing urea (5 mM), urease (1.4 U mL<sup>-1</sup>) and increasing concentrations of (a) acetic acid ( $i = 0.2$ ,  $ii = 0.58$ ,  $iii = 0.93$  mM) or (b) sulphuric acid ( $i = 0.05$ ,  $ii = 0.11$ ,  $iii = 0.18$  mM). (C) Schematic representation of the feedback mechanism in the trypsin oscillator and (D) actual molecular network. (E) Trypsin oscillations obtained with the conditions shown in the inset. Adapted with permission from (A) ref. 49, Copyright 2008, John Wiley and Sons, (B) ref. 48 Copyright 2010, the American Chemical Society, (C–E) ref. 50, Copyright 2015, Nature Publishing Group.

temporal regulation under mild conditions. Time-controlled switches in closed systems are already available, oscillators are operational in fed CSTRs, and only a few steps are missing to develop autonomous oscillatory behavior in closed reactors. Examples from synthetic biology are already paving the way.

### 2.4. Rational design of DNA-based temporal control mechanisms

In living organisms, temporal control on long time scales relies extensively on gene expression (Fig. 2F). Rather than assembling such a complex reaction network in a flask, one can introduce a sequence of genes programming an oscillatory protein expression directly in bacteria.<sup>52</sup> The “repressilator” implemented in *E. coli* consists of a plasmid with three genes, where each gene encodes a protein inhibiting the expression of the next gene, thereby providing a triple negative feedback loop (Fig. 5A). Since one of the gene expressions is also coupled with a functional output (a variant of the green fluorescent protein), the periodic increase of fluorescence in *E. coli* enables to directly monitor the oscillations with periods of around 160 min.

The introduction of a positive feedback loop in a similar system improved the robustness of the oscillations, allowing at the same time to decrease the oscillation period down to

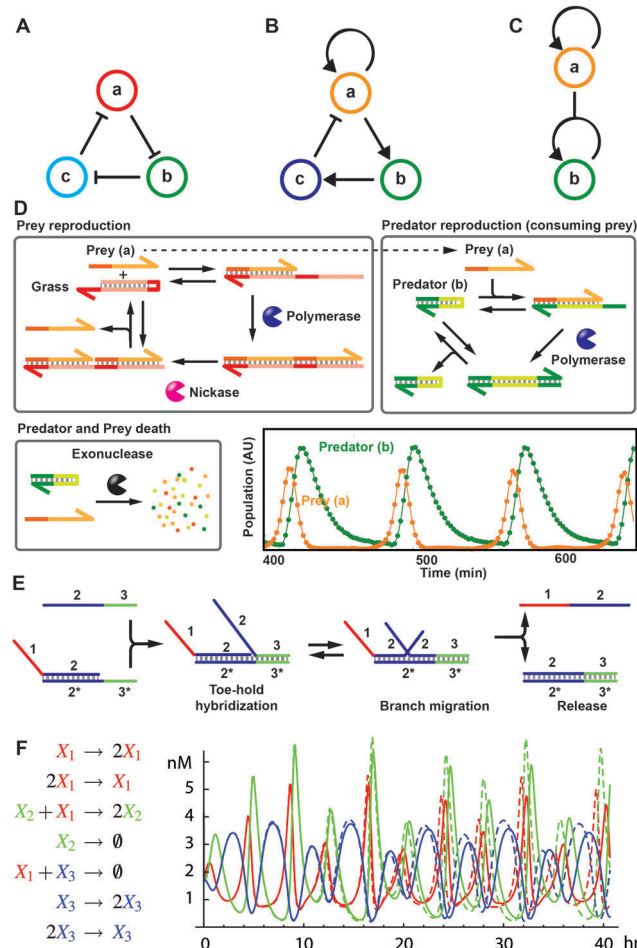


**Fig. 5** Rational network architectures for oscillatory behavior based on DNA systems. (A) The “repressilator” triple negative feedback architecture. (B) Delayed negative feedback with autocatalytic positive feedback loop. (C) A predator/prey “ecosystem”, where the predator “b” consume the prey “a”. (D) Elementary steps in the PEN toolbox applied to the implementation of a predator/prey model. Evolution of the prey and predator populations in an actual experiment (bottom right). (E) Schematized strand displacement reaction, based on toe-hold hybridization and branch migration. (F) Example of a chaotic oscillator (Rössler) implemented from strand displacement reactions. The reaction network (left) leads to chaotic oscillations (right) both in theory (dotted lines) and in experiments (full lines). Adapted with permission from (D) ref. 59 Copyright 2013, the American Chemical Society, (E) ref. 61 Copyright 2011, Nature Publishing Group and (F) ref. 62 Copyright 2010, the National Academy of Sciences.

13 min (Fig. 5B).<sup>53</sup> Such systems can be disconnected from a biological level using for instance cell-free gene expression systems embedded in microfluidic systems. Those not only enable a further control of the dynamic behavior but also a deeper understanding of the feedback processes driving the oscillations.<sup>54–56</sup>

Going one step simpler, on the DNA level, DNA nanotechnology has paved the way for the design of complex reaction networks based on enzymatic replication<sup>57</sup> or transcription.<sup>58</sup> Both principles are related and we will shortly describe the PEN system (Polymerase–Exonuclease–Nickase) based on DNA replication (Fig. 5D). The underlying network is programmed in

(exo)nuclease-resistant single-stranded DNA strands, which serve as the template for the replication by DNA polymerases. The produced copies are then cut by nicking enzymes, released in solution, and interact with complementary templates by hybridization before being eventually degraded by exonucleases. The transient DNA copies activate (positive feedback) or inhibit (negative feedback) the replication of specific templates, which enables the construction of arbitrary reaction networks for autonomous temporal control in closed systems.

This flexible platform was used to implement delayed negative feedback networks with autocatalytic amplification, leading to robust oscillations in a closed system as well as a molecular mimic of the predator/prey (fox/rabbit) ecosystem (Fig. 5B–D).<sup>57,59</sup> Controlled kinetics and custom design of synthetic DNA sequences makes the PEN system powerful to implement rationally designed dynamic networks in closed environments. A further walkthrough for the design and implementation of reaction networks can be found elsewhere.<sup>60</sup>

Towards a more simplistic control, it is also possible to remove the enzymes and implement dynamic DNA networks only using strand displacement reactions, where a partially complementary strand in a DNA duplex is replaced by another strand with a higher binding affinity.<sup>63–65</sup> In these reactions, a single strand binds to a duplex *via* a toe-hold (single-stranded segment) and initiates a reversible branch migration which ends up in the formation of the most stable duplex and ejection of the less binding strand (Fig. 5E). The dynamics of strand displacement reactions depend mainly on the presence and length of the toe-hold. The exchange rate increases over six orders of magnitudes as the toe-hold length increases (from 1 to 6 bases) before reaching a plateau.<sup>63</sup> The example in Fig. 5E shows an irreversible strand displacement as the absence of a toe-hold on the formed duplex prevents any backward reactions.

Toe-hold control allows inhibiting the strand displacement reactions by hiding toe-holds in the hybridized duplex form,<sup>66</sup> or designing catalytic strands that reveal inaccessible toe-holds (*via* a first displacement reaction) before regeneration by a later displacement.<sup>67</sup> Released strands can induce downstream displacement reactions (cascade reactions), capture catalytic strands (negative feedback) or catalyze their own release (positive feedback).

As a major advantage, sequence-defined DNA oligonucleotides enable the design of multiple strand displacement reactions that can either behave orthogonally to each other, or exert coupled feedback. Integration of such arbitrary networks of cascading strand displacement reactions allows complex system behavior, including periodic and chaotic model networks such as the Oregonator and Rössler oscillators (Fig. 5E). We will later on discuss how they can be used for motion (Section 4.2) and computation (Section 5.3).<sup>62</sup>

Consequently, it becomes obvious that the high levels of programmability in DNA-based systems provide the finest design control over temporal regulation in molecular systems at the moment, both on a gene/oligonucleotide level, as well as on a protein expression level.

### 3. Driving mechanisms and temporal behavior of autonomous structures

A key intermediate challenge for the development of autonomous devices and materials is the creation of autonomous structures. Such systems go beyond passive responsiveness to external signals by actively orchestrating dynamics (formation, steady-state, decay) and properties in time by out-of-equilibrium reaction networks and controlled internal dynamics. While such concepts are common in living organisms their synthetic design remains challenging. We will give an overview of the types of temporal behavior and some underlying principles for the design of autonomous artificial materials.

#### 3.1 Out-of-equilibrium biological structures

Cells can rapidly contract, generate protrusions, divide, move and organize internal organelles according to internal (or external) signals. Many of the internal signals are generated by the temporal control mechanisms described previously (see Section 2.1). The cytoskeleton, a network of dynamic structures, takes care of generating the appropriate response to these signals.

The cytoskeleton contains three main out-of-equilibrium supramolecular assemblies, constantly polymerizing and depolymerizing: microtubules, actin filaments and the intermediate filaments.<sup>58</sup> The microtubules, the largest of these structures, are mechanically stiff, highly dynamic, and alternate between stable growth and fast depolymerization.<sup>69</sup> They are the prototype of chemically fueled, energy-dissipating self-assembly with dynamic and adaptive properties. Microtubules consist of a tubular assembly of a hetero-dimeric protein ( $\alpha/\beta$ -tubulin) bound to a guanosine di- or triphosphate (GDP or GTP). The binding of GTP is the energy uptake step and renders the GTP-tubulin building blocks metastable. Those metastable GTP-tubulins add to the end of the microtubule and hydrolyze into GDP-tubulin soon after their incorporation (energy dissipation step). The microtubules contain therefore mostly (deactivated) GDP-tubulin, and are spun like springs, ready to undergo disassembly. Once hydrolysis reaches the tips and overcomes growth by addition of (activated) GTP-tubulin, the microtubules turn fully unstable and depolymerize rapidly (Fig. 6A). These dynamic instabilities allow for a quick reorientation and a fast search of the cellular space. Target organelles emit signals that stabilize microtubules that have found their targets. Microtubules are important for sorting the chromosomes during cell division (Fig. 6B), and also serve as tracks for molecular motors (Section 4.1) to transport large cellular components.<sup>70–73</sup>

An important feature of this dissipative self-assembly is the fact that structures only form as long as there is energy (GTP) in the system. Hence, the overall lifetime of the steady-state microtubule self-assembly (*e.g.* *in vitro*) is bound to the GTP fuel present in the system. Once all GTP is consumed, the structures decay entirely.

Taking another example from the cellular cytoskeleton, actin proteins also form dynamic polar filaments. Their assembly is based on a similar mechanism where adenosine triphosphate bound-actin (ATP-actin) monomers are polymerized at one

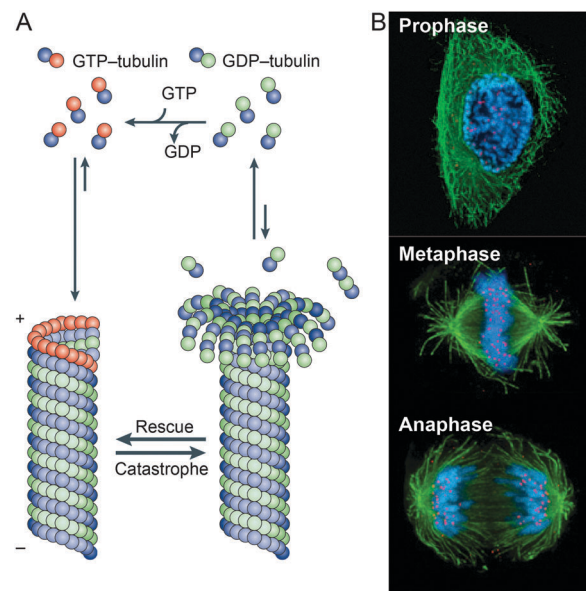


Fig. 6 Microtubule self-assembly and dynamics. (A) Schematic representation of dynamic instabilities during microtubule polymerization. (B) Immunofluorescence images showing DNA (in blue) and microtubules (in green) during human cell division. Adapted with permission from ref. 70 Copyright 2008, Nature Publishing Group.

end of the fibrils, hydrolyzed to ADP-actin and depolymerized at the other end. Actin filaments are not designed for spatial search and therefore do not switch between polymerization and depolymerization as quickly as microtubules. In contrast, their steady unidirectional growth, regulated by over hundreds of accessory proteins, provides a reconfigurable network capable of deforming the cell membrane. Actin polymerization powers for example the extrusion of filopodia allowing cell crawling and spreading. It also polymerizes as a ring at the middle of the cell during mitosis, which contracts after segregation of the chromosomes, to generate two new cells.<sup>74–77</sup>

To summarize, actin and tubulin are catalytic structural components fueled by ATP and GTP hydrolysis, respectively. They can exist simultaneously with different dynamics and regulated properties because they use orthogonal fuels. Their dissipative nature enables new functionality such as quick spatial search and autonomous reconfiguration, which are driven by two hierarchical feedback and signaling mechanisms. One at the supramolecular assembly level, which drives their dynamic growth/depolymerization, and one at the cell environment level, which regulates the global behavior (cellular re-organization, localized membrane deformation...).

Obviously such autonomous biological materials (powered by stored and on demand produced chemical fuels) are of overwhelming complexity. Discussing synthetic out-of-equilibrium self-assembling structures in the next part will hopefully dissipate some confusion and promote future advances.

#### 3.2 Principles of synthetic out-of-equilibrium temporal structures

Fueled out-of-equilibrium structures consume energy to maintain a steady-state and spontaneously disappear in the absence of it.

Examples are very diverse and range from the reversible light-induced aggregation of gold nanoparticles<sup>78,79</sup> (further description Section 3.3) to the GTP-fueled spatial search of microtubules.<sup>70</sup> Obviously, molecular mechanisms, levels of autonomy and temporal behavior differ strongly. It is therefore necessary to refine classification based on these parameters.

We identify two characteristics of out-of-equilibrium structural systems that strongly impact their functions. The first characteristic is their capacity to store energy and induce structural transitions in autonomy. We already began this discussion in Section 2 concerning homogeneous oscillators in open or closed reactors (exchanges of matter); only the latter ones can store energy and display complex behaviors in autonomy. Here, it is further important to consider the exchange of energy (light, heat, dynamic magnetic field...).

A system is truly autonomous when the temporal control is effective in isolation, that is, in the absence of exchange of either matter or energy (Fig. 7A and B). We already see here that light-driven assembly is conditioned to the ingress of light (externally powered), while tubulin systems can store energy in the form of GTP and use it on demand to work autonomously. In the case of autonomous systems, self-assembly is powered by the transformation of a chemical fuel (high chemical potential) into more stable products (Fig. 7C).

We believe that out-of-equilibrium structures will find most of their applications if they have the capacity to store energy and operate autonomously, or have energy available to adapt to external signals in an active fashion. Additionally, light is the

most attractive external regulator as it can be delivered with high spatial, temporal and energy resolution. Therefore, we emphasize on autonomous systems and light throughout this Section.

The different examples are classified primarily according to the level of complexity (the number of structural transition) that they achieve in autonomy (that is once the energy input has stopped). We will start from decay of structures that spontaneously disassemble (one transition), and then discuss transient structures that undergo successive assembly and disassembly (two transition) before looking at oscillating structures (with three or more structural transitions). This may be the most natural classification because it defines potential applications and matches the complexity of the regulatory network involved.

The second important characteristic is the nature of the active component in the system. This can either be the structural elements themselves or the environment. The active component of the system is the one in charge of harnessing the energy by fuel conversion.

In Section 2 we discussed the temporal regulation of chemical potentials in solution. These can actually serve as active environments to generate out-of-equilibrium structural systems. To create such systems one needs to choose a responsive structural element that is actuated by the temporally controlled chemical potential. In contrast, in systems with active structural components (*e.g.* tubulin), the latter can directly catalyze the consumption of the fuel present in the environment (GTP hydrolysis) to drive their autonomous behavior.

This difference has a strong impact on the system behavior. Active environments promote the synchronous actuation of all the structural elements in the system, necessarily leading to the corresponding macroscopic effect (gelation, dissolution...). In contrast, systems driven by active structural elements can sustain persistent macroscopic properties (self-healing, reorganization, homeostasis...) but can feature continuous assembly/disassembly of the underlying structures (Fig. 7D).

### 3.3 Decay of metastable and steady-state structures

The simplest autonomous behavior of an out-of-equilibrium system is the spontaneous transition from a high energy state to a state of lower total energy.

Relaxation events and transitions occur in any responsive material where the application of a stimulus, hence a change in the thermodynamic environment, leads to the induction of a new equilibrium structure. Metastable structures are obtained when the transient state persists in time (without fuel consumption). The decisive time-scale coupled to this process relates to the kinetic bottlenecks or the activation energy of the pathway to fulfill the transition. Thermal energy or an external chemical trigger is needed for metastable structures to reach thermodynamic equilibrium. It is possible to control the time-scale of such a process by modification of the molecular structure or the thermal energy available. In this context, kinetic structural control based on enzymes,<sup>80</sup> supramolecular assemblies,<sup>81</sup> dynamic building blocks<sup>82–84</sup> or reaction-precipitation<sup>85,86</sup> are exciting tools to prepare new nano- and

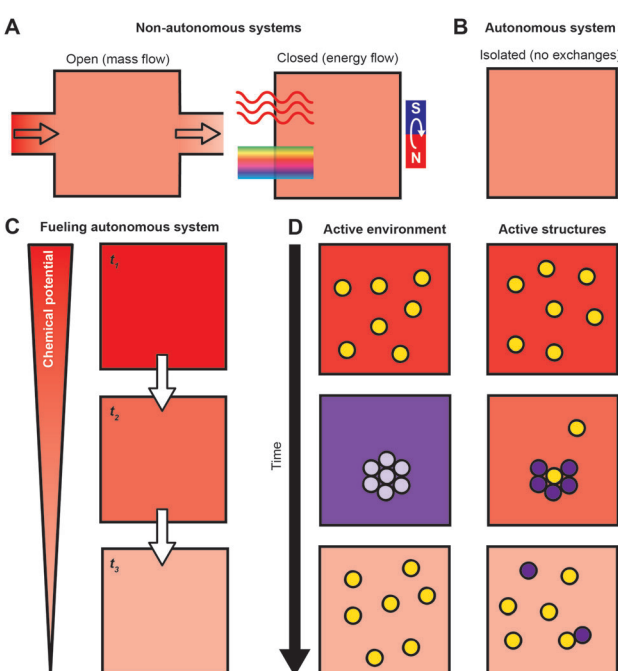


**Fig. 7** Classification of out-of-equilibrium structural systems. Schematic representation of (A) open and closed non-autonomous dissipative systems and (B) an autonomous isolated system. (C) The decrease of chemical potential in an autonomous chemical system. (D) Molecular representation of autonomously transforming structural systems driven by an active environment (left) or active structures (right).

microstructures with complex shapes and observable time scales and transitions. We also point to controlled degradation of hydrogels<sup>87–89</sup> or self-immolative polymers<sup>90</sup> which are at a relevant interface between responsive and metastable systems.

Fundamentally different from such kinetically trapped systems are far-from-equilibrium, energy-dissipative systems, which require a constant energy supply to maintain a form of organization (Fig. 8A). A seminal example deals with magnetic discs floating at the surface of water and which are powered by a rotating magnetic field to form steady-state patterns.<sup>91,92</sup> The regular organization of the discs disappears as soon as the magnetic field stops rotating. The decay of this structure can be considered an autonomous process, where, similar to above, the relaxation to a thermodynamic ground state appears.

More advanced molecular mechanisms are encountered in light-driven systems. Light can interact with many molecular systems (absorption) and can be precisely controlled in time, space and intensity. It is hence an energy source of choice to start with the design of out-of-equilibrium self-assemblies.

We first focus on active environments (Fig. 7D). It is for example possible to create light-fueled self-assemblies by combining a pH-responsive system with reversible photoacids or photobases present in the environment. For instance, malachite green is an efficient photobase, which releases a hydroxide ion upon UV-irradiation and re-captures it when light is stopped.<sup>93</sup> This photoswitch was used to drive the opening of the pH-responsive DNA i-motif,<sup>94</sup> and to create light-fueled hydrogels.<sup>95</sup> Similarly, spirocyclic derivatives can release protons upon irradiation and recapture them in dark, which were used to drive supramolecular and nanoparticle self-assembly (Fig. 8B).<sup>96,97</sup>

Interestingly, spatial patterning using masks can create pH-gradients in solution.<sup>97</sup> The equilibration of the pH gradient once the irradiation is stopped can then be used to prepare self-erasing patterns in hydrogels containing pH-responsive nanoparticles (Fig. 8D).

Note that these examples are instructive to point to the often unclear boundaries between classical acid/base triggered systems, where a trigger changes the situation infinitely in closed systems, and self-reverting, energy-sustained systems where a change is only maintained under continuous external energy input. The systems discussed above are interesting because the environment is driven out-of-equilibrium by constant energy uptake, and the structural element, material or molecular switch follows. Once the energy supply is switched off, even in a closed system, the system will return to the ground state with a time delay defined by the reversing process (Fig. 8A).

The previous examples are typical of an active environment, as the photosensitizer (malachite green/spirocyclic) does not take part in the self-assembly process. However, light can also be used as a direct dissipative switch to trigger photoactive structural components while leaving the environment unmodified (Fig. 7D). Such light-driven materials rely on molecular photo-switches that revert back to their original state spontaneously. Azobenzenes are possibly the best understood molecules and undergo UV-induced isomerization resulting in an unstable *cis*-conformation that spontaneously returns to the thermodynamically more stable *trans*-conformation. The *cis-trans* isomerization modifies the dipole moment of the azobenzene molecules and creates molecular motion. These are the two main effectors to impose changes on structures.

Azobenzenes have had a strong impact on realizing photo-responsive actuators based on liquid crystalline elastomers in bulk (Fig. 16A),<sup>98,99</sup> and for manipulating self-assemblies in solution.<sup>100,101</sup> For instance, gold nanoparticles partially covered by azobenzene derivatives aggregate under UV-irradiation in organic solvents due to changes in the polarity (Fig. 8C). Since the absorption spectra of the *trans* and *cis* isomers overlap substantially, continuous irradiation produces typically a photo-stationary state with a maximum of ca. 80% *cis*.<sup>102</sup> This gives rise to annealing of the structures due to constant switching in the steady-state. Such gold nanoparticle lattices spontaneously disassemble when the light is switched off.<sup>103</sup>

Changing the nature of the azobenzene derivative creates nanoparticles that selectively aggregate at different wavelengths.<sup>104</sup> The first self-erasing nanoparticle patterns were actually made

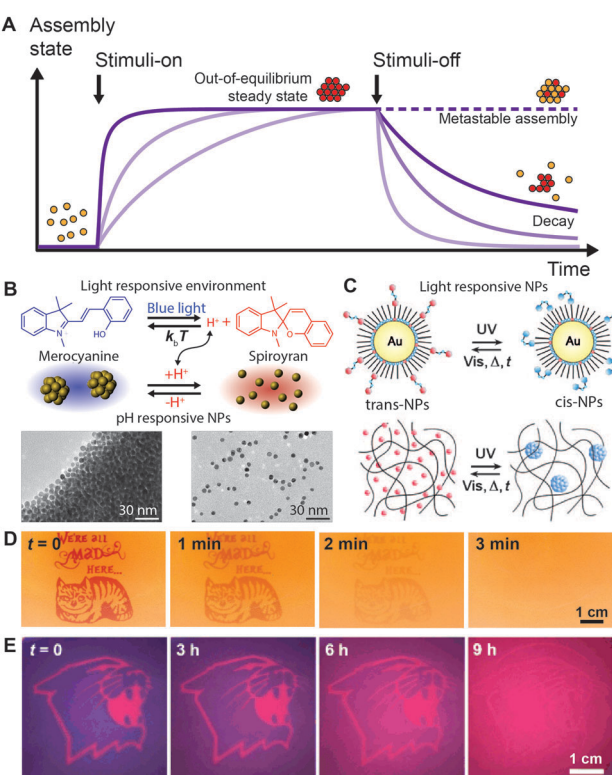


**Fig. 8** Autonomously decaying structures. (A) Temporal behavior of stimuli induced assembly regarding the speed of formation and the structural stability. Active environments: (B) schematic representation of blue-light-induced aggregation of pH-responsive nanoparticles associated with the photoinduced merocyanine to spirocyclic transformation, which releases protons. (D) Self-erasing image due to the spontaneous reaggregation of blue light dispersed pH responsive NPs. Active structures: (C) schematic representation of UV-induced aggregation of azobenzene-decorated Au-NPs. (E) Self-erasing images due to the spontaneous decay of the azobenzene-decorated Au-NP aggregates. Adapted with permission from (B and D) ref. 78 Copyright 2015, Nature Publishing Group and (C and E) ref. 79 Copyright 2009, John Wiley and Sons.

from such azobenzene-decorated nanoparticles dispersed in an organogel (Fig. 8E),<sup>79</sup> and recent work suggested the use of transiently formed nanoparticle crystals as nanoflasks to accumulate chemicals and bias reactions.<sup>105</sup>

Towards an engineering of the relaxation time-scale once the energy input is stopped, it is possible to change the type of azobenzene (as derivatives have different thermal half lives<sup>102</sup>) or the azobenzene coverage on the gold nanoparticles.<sup>79</sup>

### 3.4 Transient self-assemblies with active environments

Autonomous materials with a controllable lifetime require chemical fuels and orchestrated chemical reaction networks to maintain a time-programmed functionality. As discussed in Section 3.1 such transient states can either be obtained by targeting active structural elements in a relatively constant environment, or in a system approach by coupling responsive self-assemblies to an active environment (Fig. 7).

Towards the latter approach, we recently developed a generic concept to create time-controlled pH transitions that can be coupled to virtually all pH-responsive systems to generate transient self-assemblies.<sup>49,106</sup>

The developed pH control system consists of a combination of a fast acting alkaline buffer (alkaline TRIS buffer as promoter) with a simultaneously added ester (dormant deactivator) that spontaneously hydrolyzes (with pH-dependent speed) in water to form a carboxylic acid (time delay). The direct availability of the alkaline buffer first increases the pH and the slow and pH-dependent, non-linear hydrolysis of the ester restores the original pH levels. Once coupled to a suitable pH-responsive self-assembling system, it is possible to regulate their lifetimes by superimposing the two pH actuating systems. Since the pH-driving environmental system and the building blocks are coupled, a part of the chemical potential (extent of the pH-jump) is consumed by the coupled building blocks. The strongest effect on the regulation of the timescale of the transient structures is provided by the hydrolytic stability of the used ester. The amount/ratio of ester and buffer then fine-tunes the lifetime of the self-assemblies with time scales from minutes to days. Using this system it was possible to successfully program the temporal stability ("lifetimes") of transient oligopeptide, nanoparticle and block copolymer self-assemblies (Fig. 9C and D).<sup>106</sup>

Other approaches to control lifetimes by modulation of a signal include for instance slow degradation of a complexation agent using enzymes to shift the equilibria of supramolecular assemblies and create transient fluorescence signals<sup>107</sup> or self-assembled vesicles.<sup>108</sup>

We recently realized a more advanced, biocatalytic feedback-driven transient state at low pH by combination of the urease/urea switch (Fig. 4A) with an acidic buffer (activator). The duration of the transient acidic profile can be controlled by changing the urease concentration driving the feedback-regulated pH reversal (dormant deactivator). Coupling of this transient acidic state to peptide hydrogelators, forming solid gels at low pH, enabled the generation of the first time-programmed hydrogels with widely tunable lifetimes ranging from a few minutes to several hours (Fig. 9E). Those autonomously self-regulating hydrogels have been

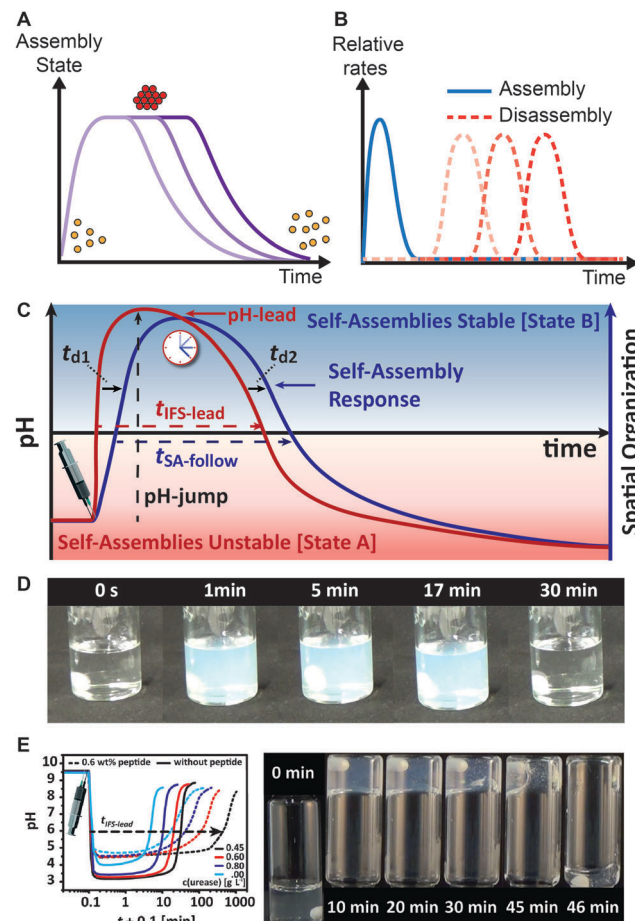


**Fig. 9** Transient structures driven by an active environment involving pH feedback systems. (A) Temporal behavior of the assembly as function of the amount of activator/dormant deactivator and (B) the corresponding assembly and disassembly rates of the structural elements. (C) Scheme for the temporal regulation of pH-responsive assemblies using such internal pH feedback systems. (D) Photographs showing the transient formation of vesicles by a pH-responsive block copolymer, as indicated by the turbid dispersion. (E) Opposite transient acidic pH profile obtained by combining urease/urea with an acidic buffer, and its application to the temporal control of a peptide hydrogel assembling at low pH. Adapted with permission from (C and D) ref. 106 Copyright 2014, American Chemical Society, and (E) ref. 49 Copyright 2015, John Wiley and Sons.

proven to be useful to temporally block microfluidic channels and reroute fluid flow in simplistic vascular network models for a pre-programmed time.<sup>49</sup>

In the examples above, temporal control relies on the modulation of the chemical environment of responsive structural elements that drove their assembly and disassembly. This concept allows a robust implementation of temporal control mechanisms based on well-understood responsive structures. It however cannot reproduce the dynamic behavior of microtubules or actin filaments, as all responsive building blocks switch in a synchronized fashion with the environment (Fig. 9A and B). Even though dynamics occur between activation and deactivation of building blocks (as it does in all acid/base responsive systems), they are unlikely to be of similar subtlety as found in the kinetic balance of microtubule self-assembly featuring dynamic instabilities.

### 3.5 Transient self-assemblies from active structural elements

Autonomous materials made of active structural components are closer to biological systems, and may lead to new functionalities arising from the concurrent assembly and disassembly processes (Fig. 10A and B). One of the most interesting long term prospects could be in the direction of multicomponent systems with orthogonally self-assembling active, dissipative elements, such as actin (ATP-driven) and microtubule (GTP-driven) in cells, able to perform independent tasks in a single environment. Hence there is profound interest in making transient self-assemblies based on active structural components using specific and selective fuels.

Peptide modifications by enzymatic reactions represent one promising approach to create dynamic building blocks with potentially high selectivity.<sup>89</sup> Chymotrypsin was for example used to catalyze the formation and dissolution of transient peptide hydrogels. Chymotrypsin catalyzes the rapid *trans*-acylation of a soluble methyl-ester gelator precursor to form an aromatic dipeptide that forms fibrils and gels the system. It also catalyzes the slower hydrolysis of the (just formed) gelator to its soluble carboxylate form, thereby driving a time-delayed disassembly of the structure.<sup>109</sup> The lifetime of the transient hydrogel can be modulated by the amino acid sequence of the gel-forming

peptide.<sup>110</sup> It is interesting to note that the gelator precursor is the fuel (high energy chemical consumed during the reaction) while the enzyme is indeed the catalytic unit. Re-initiating the self-assembly involves the addition of more gelator precursor, which limits the number of cycles the system can undergo.

In a chemically triggered system, methyl ester-based hydrogels were generated *in situ* from soluble carboxyl-containing precursors using different methylation agents (methyl iodide<sup>111</sup> or di-methyl sulphate<sup>112</sup>). Under alkaline conditions the methyl ester groups are however prone to spontaneous hydrolysis back to their soluble carboxylic form by hydroxide ions.<sup>111</sup> At a sufficient concentration of the methylation agent and at an appropriate pH, it is possible to reach a steady-state of methylated gelators that form self-assembled fibrils and even hydrogels while consuming the methylation agents. Here, the system is based on a reusable active structural component that is driven out-of-equilibrium by a chemical fuel (methylating agent, Fig. 10C). More importantly, the supramolecular fibers show simultaneous assembly (fuel uptake) and disassembly (hydrolysis) microscopically, while maintaining a macroscopic integrity – a behaviour quite reminiscent of that of microtubules (Fig. 10E and F).

Such fuel-driven instabilities also provide a new mechanism for self-healing, as the constant re-organization of the network autonomously repairs damaged areas (Fig. 10D).<sup>112</sup> The study sets a benchmark for autonomous systems built from active structural components, but the necessity to develop systems relying on less toxic fuels and operating at physiological pH leaves plenty of room for future developments.

Furthermore, autonomously transforming materials with complex temporal behavior beyond peptide self-assemblies and in particular approaching multiple macroscopic transitions would also be attractive.

### 3.6 Oscillating structures

In Section 2 we reviewed how feedback-regulated reaction networks can generate oscillating chemical potentials. We will now connect these principles to driving interactions in structural components to reach dynamic structures (Fig. 11A and B). Again we will learn about system approaches with building blocks and environments being in synchronized behavior, and about active building blocks within a relatively steady environment.

As discussed in Section 2.2 the BZ reaction has been established as a reliable workhorse to study long lasting redox oscillations in closed systems. To create an autonomous material driven by this reaction, it needs to be coupled to redox-responsive structures with a suitable potential window. A major breakthrough was achieved for poly(*N*-isopropyl acrylamide) hydrogels (PNIPAM) with covalently bound ruthenium tris-(2,2'-bipyridine) catalysts (replacing the cerium described in Section 2.2).<sup>41</sup> In the presence of the BZ system the ruthenium catalyst oscillates between the reduced ( $\text{Ru}^{2+}$ ) and oxidized form ( $\text{Ru}^{3+}$ ), promoting the shrinking and expansion of the hydrogel due to the charge modification of the polymer backbone (which shifts the volume phase transition temperature of the modified PNIPAM below and above the working temperature). The key is to directly bind the catalytic redox center to the polymer to create an active compound central to the oscillatory mechanism.

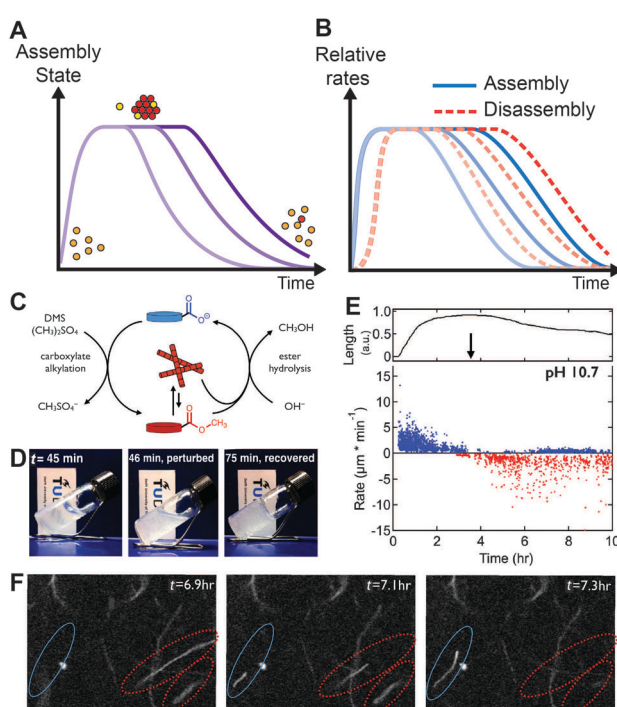


**Fig. 10** Transient structures using active structural elements. (A) Macroscopic temporal behaviour of the assembly as a function of the amount of fuel introduced and (B) the corresponding assembly and disassembly rates of the structural elements. (C) Schematic model for the mechanism of fibril formation with active building blocks where methylation and hydrolysis compete. (D) Photograph of the self-healing properties of the gel. (E) Length and relative growth rate of individual fibrils measured by confocal microscopy. (F) Confocal visualization of the simultaneous growth and shrinkage of the fibrils at pH 10.7. Image length is 30  $\mu\text{m}$ . Adapted with permission from (C–F) ref. 112 Copyright 2015, the AAAS.

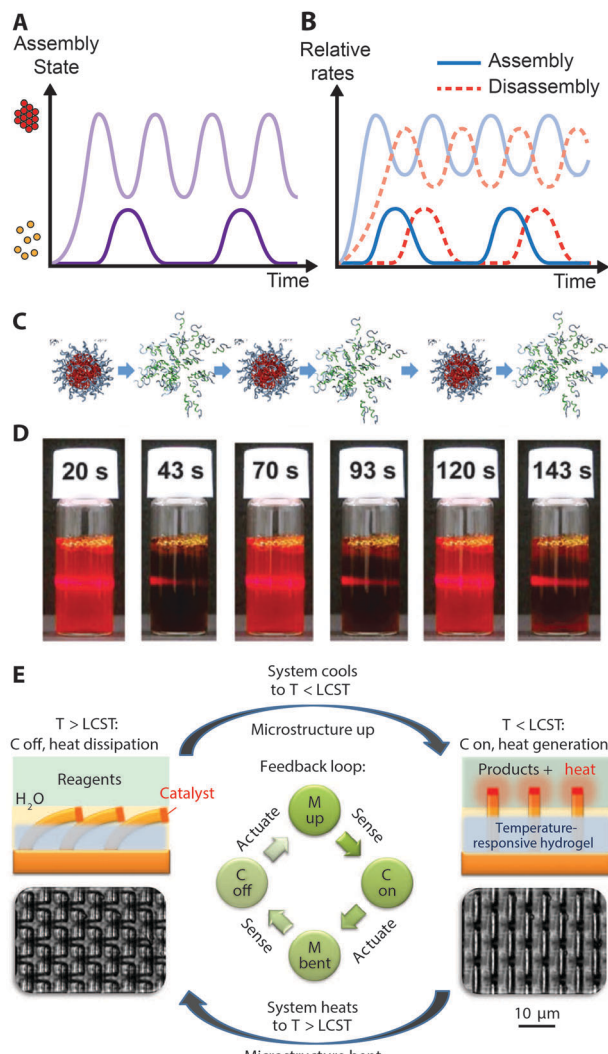


**Fig. 11** Oscillating structures. (A) Macroscopic temporal behavior of some oscillatory structures and (B) the corresponding assembly and disassembly rates of the structural elements. (C) Scheme of self-oscillating micelles. (D) Variation of turbidity associated with micelle formation. (E) Chemo-mechano-chemical oscillations of rigid posts embedded in a temperature responsive hydrogel. The catalyst at the top of the posts contacts the reagents, leading to heat-up and subsequent bending of the posts into the reagent free layer until the temperature drops to reinitiate a cycle. Adapted with permission from (C and D) ref. 114 Copyright 2013, the Royal Chemical Society, and (E) ref. 127 Copyright 2012, Nature Publishing Group.

Due to the feedback mechanisms involving soluble intermediates with fast diffusion coefficients (bromous acid and bromide) the systems undergo synchronous transitions in well-stirred polymer solutions or microgel suspension, but as we will see in Section 4.4, reaction/diffusion fronts with coupled volume changes occur for unstirred systems with large dimensions.

Based on this principle several autonomous materials were developed, *e.g.*, a polymer dispersion undergoing rhythmic solubility/insolubility transitions,<sup>113</sup> a block copolymer periodically assembling into micelles (Fig. 11C and D),<sup>114</sup> microparticles spontaneously flocculating and dispersing,<sup>115</sup> or microgel suspensions with oscillating viscosity.<sup>116</sup>

In parallel, several examples of oscillating structures and materials emerged by coupling of pH-responsive elements with pH oscillators. Direct actuation of pH-responsive hydrogels led to materials that swell periodically,<sup>117–119</sup> gold or silver nanoparticles decorated with pH-responsive ligands presented oscillatory aggregation,<sup>120</sup> carboxylic acid surfactants showed rhythmic micelle-to-vesicle transitions,<sup>121</sup> and pH-responsive i-motif DNA sequences switched periodically from the canonical duplex to the intermolecular quadruplex.<sup>122–124</sup> One should however note that these examples differ from the active BZ-based materials because they consist of responsive structures driven by an active environment, and are not involved directly as a catalytic species in the original reaction network. The pH-induced collapse of a responsive hydrogel can nevertheless induce an additional feedback mechanism as proton diffusion in the hydrogel differs in the swollen and collapsed states. A hydrogel system exploiting this feedback displayed oscillatory behavior in a static environment.<sup>125,126</sup>

Another sophisticated oscillatory system was built by embedding epoxy posts with a catalyst at their top into a thermo-responsive hydrogel, so that the tips stick out of the hydrogel. Below the critical temperature for the volume phase transition of the hydrogel, the catalyst posts are in contact with their substrates (in a microfluidic setup) and produce heat due to an exothermic reaction. The heat generation induces the collapse of the hydrogel, and the posts bend downward, thereby separating the catalysts from their substrate. The interruption of the exothermic reaction subsequently causes the temperature to drop, which reinitiates the cycle as the catalyst at the tip of the posts is re-exposed to its substrate when the hydrogel re-swells. The time-delay in thermal equilibration and the hysteresis of swelling the polymer network contribute in establishing robust oscillations (Fig. 11E).<sup>127</sup> This example is particularly interesting as chemical reactions, complex hybrid structures, thermal transport and the hysteresis of a polymer network are all combined in a functional microfluidic system.

Towards biomolecular oscillating systems, we described above how DNA systems enable high levels of programmability and operation in an autonomous fashion, and therefore open considerable opportunities for precise materials design. For instance, the transcription oscillator discussed in Section 2.4 was used to actuate DNA-tweezers.<sup>58</sup> Since opening and closing the DNA tweezers consume some of the interacting strands driving the oscillatory network, they act as load on the system and damp the oscillations. Depending on the position in the network where the load is applied (and on the amount introduced), the responsive tweezers can completely prevent the system from oscillating.<sup>128</sup> Unlike previous examples for pH driven systems,<sup>120,122</sup> here the amount of responsive structures is comparable to the interacting species driving the oscillations. However, the addition of insulating network features acting as an intermediate between the transcription oscillator (temporal control) and the load (responsive structural elements) assisted in making the system practically load-insensitive.<sup>128</sup>

Such components increasing the robustness of out-of-equilibrium systems will certainly play an important role in future autonomous materials where responsive structures are driven by autonomous reaction networks.

## 4. Motion and work generation

The ability to move is one of the most fascinating properties of living organisms. Motion requires energy that is converted into work by biological molecular motors, which are optimized for specific functions, such as intracellular transport, micro-propulsion or macroscopic motion. Those motors convert chemical energy in mechanical work with an efficiency close to the one of our thermal engines.<sup>129</sup> While there is a profound understanding of the underlying mechanisms in biology, translating the principles into synthetic, chemically fueled, molecular systems remains one of the grand challenges.<sup>130</sup>

We will review here the mechanisms driving fueled motion from the molecular to the macroscopic scale in biological and synthetic systems, and place an emphasis on distinguishing molecular switches from molecular motors, and derive some implications for autonomous systems in general.

### 4.1 Motion mechanisms in biology

Molecular motors convert a chemical fuel to mechanical work to control many cellular functions. They power the active transport of cargo in the cytoplasm, regulate the mechanical properties of the cytoskeleton, power flagellar propulsion of bacteria and are at the origin of muscular contraction for macro-scale movement. The challenges to achieve powered motion depend on the involved length scales, and understanding some of the solutions evolved in biology can guide the design of efficient artificial systems.

At the nanoscale, organelle transport is powered by processive molecular motors, such as kinesin that uses microtubules as tracks. Those motor proteins consist of a globular motor head containing a microtubule binding sequence and an ATP binding sequence attached to a tail domain that binds to the cargo.<sup>131</sup> Conventional kinesin walks along the microtubule by forming dimers where the two heads work in a coordinated fashion.<sup>132</sup> ATP binding to the forward head of the kinesin motor creates a twisting motion in the neck linking the two sub-units, moving the rear head forward. ATP is hydrolyzed to ADP while the head brought forward binds to the microtubule, and ADP is released. ATP binding in the front head will then initiate a new 8 nm step (Fig. 12A).<sup>133–135</sup> Coordinated motion of the two heads and constant contact with the microtubule enables the directed displacement of cargoes on long distances. The direction of the motion relative to the asymmetry of the microtubule track is directed by the chirality of the neck-coil.<sup>136</sup>

In fluids motion cannot rely on solid tracks to fight random Brownian noise. As the mass to surface ratio decreases, inertia also becomes insignificant compared to viscous drag. This renders reciprocal, time-symmetric movements such as simple flapping useless.<sup>137</sup> Bacteria like *E. coli* swim by rotating a left-handed chiral filament with a rotary motor, the ATP-synthase. Time symmetry is broken by the chirality of the flagella. Counterclockwise rotation of the ATP synthase fueled by a trans-membrane proton gradient pushes the bacteria in the direction opposed to the flagella, while clockwise rotation promotes chaotic movement, called tumbling, as the chirality of the flagella and of the rotation

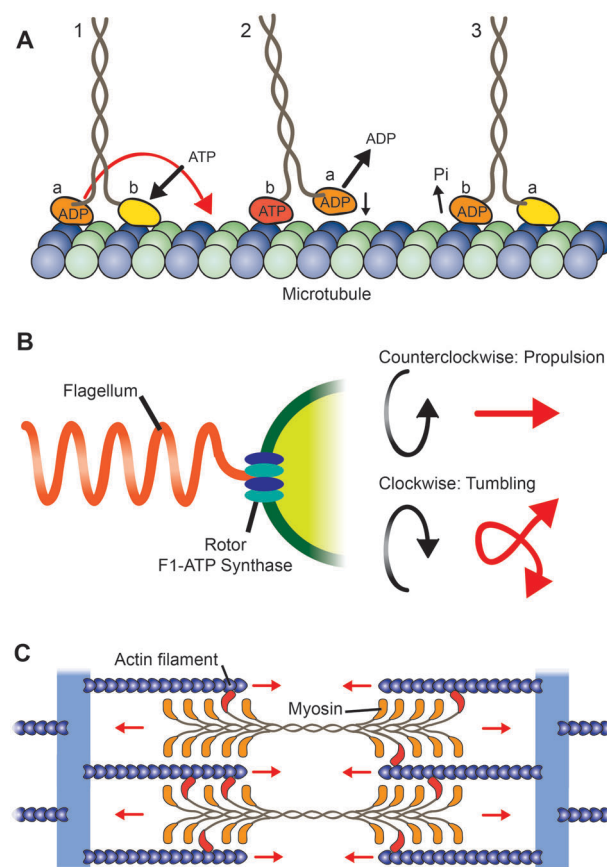


Fig. 12 Biological motion. Schematic representation of (A) the coordinated walk of kinesin motors on microtubules fueled by ATP hydrolysis, (B) the flagellar propulsion of bacteria and (C) the organization of myosin motors and actin filaments in the muscle sarcomere. Adapted with permission from (A) ref. 133 Copyright 2000, the AAAS.

are opposed (Fig. 12B).<sup>138–140</sup> We will also see in Section 5.1 how bacteria use alternating linear motion and random reorientation to direct itself in chemical gradients.

Nature has evolved other ways to generate asymmetry at the nanoscale for propulsion. For example listeria bacteria move inside the cytoplasm of eukaryotic cell by recruiting protein complexes promoting the assembly of actin fibrils. The energy released by the localized actin polymerization propels the bacteria in the direction opposed to the polymerizing actin,<sup>141,142</sup> a strategy that has also been used by some viruses.<sup>143</sup>

To summarize, propulsion in fluids requires an asymmetric distribution of forces on the objects, either created by non-reciprocal motion or by a localized reaction.

Harnessing the individual motion of thousands of molecular motors to generate macroscopic movement on the other hand requires synchronization in space and time. In muscle sarcomeres, myosins are threaded in thick-filaments interdigitized with actin fibrils.<sup>144</sup> Myosins are ATP-fueled molecular motors similar to kinesin that use actin as tracks (instead of microtubules). In contrast to kinesin, muscular myosins only bind to actin filaments for a short time, and motion is induced by the twisting of a lever arm generating a forward stroke transferred to the

filament before unbinding.<sup>133,145</sup> Coordinated series of strokes orchestrated in space by the sarcomere organization and in time by calcium signaling enables fast and large scale contraction (Fig. 12C).<sup>146</sup> This is indeed one of the most exquisite motion mechanisms as it requires both temporal and spatial synchronization at several hierarchical levels.

One possible strategy to power micro- or nanoscale motion is to extract and purify biological motor proteins and drive new out-of-equilibrium functions in man-made biohybrid material systems, as also reviewed recently.<sup>147–152</sup> Yet, most of the mechanisms at the origin of the behavior hide inside these purified motors. In order to draw essential concepts and foster the development of new synthetic materials we focus here only on the synthetic design of work-generating modules.

#### 4.2 Atomically precise motors and walkers

Classical organic chemistry has been one of the drivers towards molecularly defined machinery.<sup>153,154</sup> Right at the beginning of this Section it is important to insist on the key conceptual difference between a molecular switch and a molecular motor. Only the latter are able to accumulate work under continuous cycling, while switches mostly induce reversible changes in matter.<sup>130</sup> For example, a rotaxane moving on a thread between two positions depending on the system state represents a switch. There is no accumulation of work in a cycle as returning the switch to its initial position opposes the work generated by the first switch (Fig. 13A).<sup>155</sup> On the other hand, a molecular motor accumulates work as it returns to its original state *via* a non-identical pathway (Fig. 13B).

At least three intermediate states are necessary to create a non-reciprocal cycle of switches capable of returning to their initial position while accumulating work. Systems consisting of catenanes rotating unidirectionally along a macrocycle with three (or more) binding sites (Fig. 13C),<sup>156</sup> an unidirectional four-step rotating motor,<sup>157</sup> and a three-step supramolecular linear pump have been demonstrated.<sup>158</sup> Yet these systems rely on extensive external triggers to perform a cycle because each step requires the addition of a specific fuel. Even though they clearly present a work-generating mechanism, these structures are multi-responsive rather than autonomous and continuous as actual motors.

Some of the most promising molecular motors consist of light-powered molecules that rotate unidirectionally along a central double-bond upon UV irradiation.<sup>159</sup> The four-step rotation consists of two UV-induced *cis-trans* isomerization and two thermal relaxations. The presence of at least one stereogenic center enables uni-directional rotation (Fig. 13B).<sup>160,161</sup> The speed and direction of rotation can be modified by changing the structure of the molecular motor.<sup>162–164</sup> Another recent example deals with the light-powered unidirectional translation of a linear molecule through a macrocycle, providing new opportunities for linear transport (Fig. 13D).<sup>165</sup> The first examples of synthetic machines harnessing the work of molecular motors to create motion are also emerging. A striking example is the molecular car whose four wheels consist of the rotating motors described above. After evaporation on a copper surface the cars can move linearly with 0.6 nm steps upon electrical excitation. Efficient

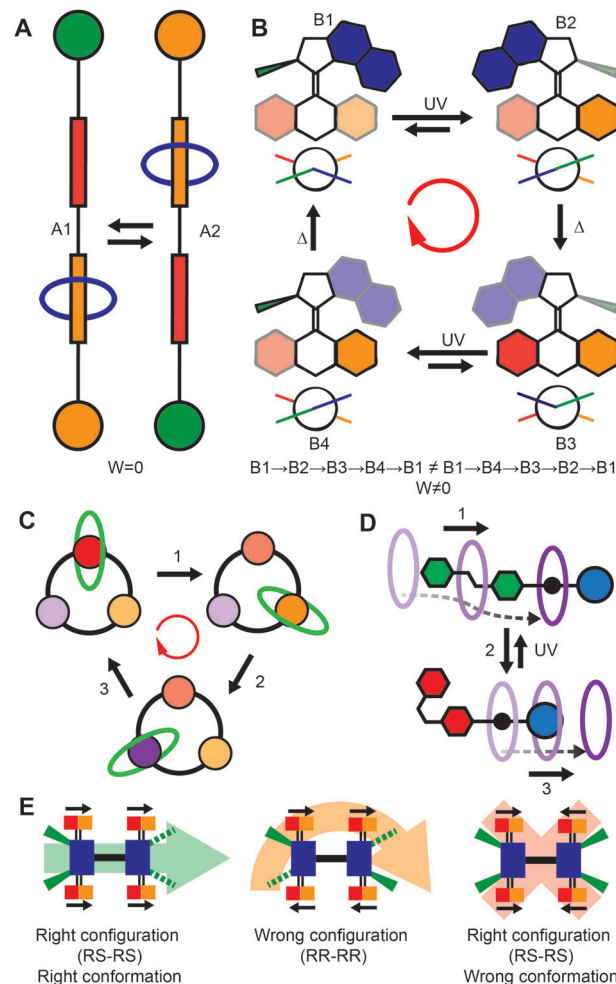


**Fig. 13** Molecular machinery: synthetic molecular motors (vs. synthetic switches). (A) Schematic representation of a reciprocal supramolecular transition that does not generate work in continuous operation: a molecular switch. (B) Schematic representation of a non-reciprocal isomerization cycle capable of generating work: a molecular motor. (C) A catenane rotating unidirectionally along a macrocycle. (D) Light powered uniaxial translation of a linear molecule through a macrocycle. (E) Molecular cars with various configuration and conformation showing either linear motion (left), random motion (center) or no motion (right) upon electrical excitation (note that while the molecular structures differ we matched the colors with structures in B to simplify understanding). Adapted with permission from (A) ref. 155 Copyright 1991, the American Chemical Society, (B) ref. 161 Copyright 2008, the American Chemical Society, (C) ref. 156 Copyright 2003, Nature Publishing Group, (D) ref. 165 Copyright 2015, Nature Publishing Group, and (E) ref. 166 Copyright 2011, Nature Publishing Group.

driving requires the four motors to work in a coordinated fashion. Cars with improper configurations (synthesis) or conformation (landing on the copper surface), respectively, show random walk or no motion at all (Fig. 13E).<sup>166</sup>

While light-powered motion offers neat access to spatio-temporal external modulation of the motors, truly autonomous systems would require harnessing chemical energy in a coordinated fashion. Steps in this direction are for instance taken by molecular walkers, which use chemical energy to power motion at the nanoscale. In solution the work generated by motor systems is

lost, hence, molecular walkers use tracks to prevent Brownian randomization and accumulate work. While chemically fueled, entirely synthetic, molecular walkers (based on organic chemistry) remain a challenge,<sup>167,168</sup> it is possible to build such walkers from DNA based on the addressability and dynamic nature of the Watson–Crick hybridization.<sup>169,170</sup>

To create an autonomous DNA walker it is necessary to drive the stepwise motion with a fuel and a catalytic unit.<sup>171</sup> The burned bridge mechanisms are most popular to drive DNA walkers because of their relative simplicity. In such systems the track serves as a metastable fuel and the walker catalyzes its transformation. An example of such a mechanism is presented in Fig. 14A. The track consists of an array of single-stranded DNA (containing an RNA base outlined in pink) while the walker consists of a DNA strand complementary to track and possessing a catalytic loop (called DNAzyme; outlined in green).

In the presence of magnesium the DNAzyme is able to hydrolyze the ribose base of the track strand, creating a small fragment (top) that melts away to reveal a toe-hold. The walker then moves to the next intact track position by first hybridizing its dangling free end to the next available DNA track strand (toe-hold hybridization) and subsequent branch migration to maximize hybridization in a single DNA duplex (see also Fig. 5). The process then restarts as the DNAzyme hydrolyzes the intact ribose base present on the newly formed duplex.<sup>172,173</sup> Instead of a DNAzyme, it is also possible to build a mechanistically similar walker using an external nicking enzyme. The nicking enzyme replaces the DNAzyme and the track does not require a RNA base, because the enzyme can recognize and hydrolyze regular DNA strands.<sup>174</sup>

Such track-fueled mechanisms promote an unidirectional motion as the walkers always move towards regions with intact tracks. Multipedal “spiders” with DNAzyme legs, walking according to the same mechanism, were able to follow programmed paths of ribose-containing strands created on an otherwise unexplorable DNA tile (Fig. 14B–D), demonstrating possibilities to spatially orchestrate the movement.<sup>175</sup> Similarly, it was possible to observe the motion of DNAzyme-coated nanoparticles on carbon nanotube tracks,<sup>176</sup> of enzyme-powered DNA walkers on DNA tiles,<sup>177</sup> and of rolling DNA-particles on RNA surfaces.<sup>178</sup>

Other track-fueled mechanisms have been proposed where the walker catalyzes the hybridization of a hairpin fuel with the single-stranded tracks,<sup>179</sup> which opens up possibilities to direct the motion by the nature of the fuel,<sup>180–182</sup> or to build motors with coordinated legs.<sup>183</sup>

To summarize, in order to generate work at the molecular scale it is necessary to build a cycle of switches (3 or more) that is non-reciprocal. Most synthetic machines still rely on external actuation to power such cycles while autonomous devices require a catalytic unit to convert the energy stored in a metastable fuel (structure) into work. This is the case for track-fueled DNA-based walkers, a well-established system promoting directional motion based on the burned bridge strategy. Contrary to the motion of myosin and kinesin motors, which use outside fuel, track-consuming mechanisms prevent reusability. Hence, long-range motion of solution-powered walkers leaving their track intact remains a milestone objective, but probably not for long.<sup>184,185</sup>

#### 4.3 Breaking symmetry in fluids for motors

Bacteria swim in fluids by rotating their chiral flagella, which creates an asymmetric fluid flow and propels the organism. Some synthetic devices have been built on the same principle,<sup>186</sup> however, due to their complexity, no chemically fueled motors based on such mechanisms exist. Yet much more simplistic systems have been conceived to break the symmetry of objects and create a fueled motion.

The underlying propulsion mechanisms fall in two main categories: either the objects carry the fuel on board (we will call them internally fueled motor, a macroscopic example would be a rocket) or they catalyze the transformation of a metastable fuel (we will call them catalytic motors, a macroscopic example would be a solar car).

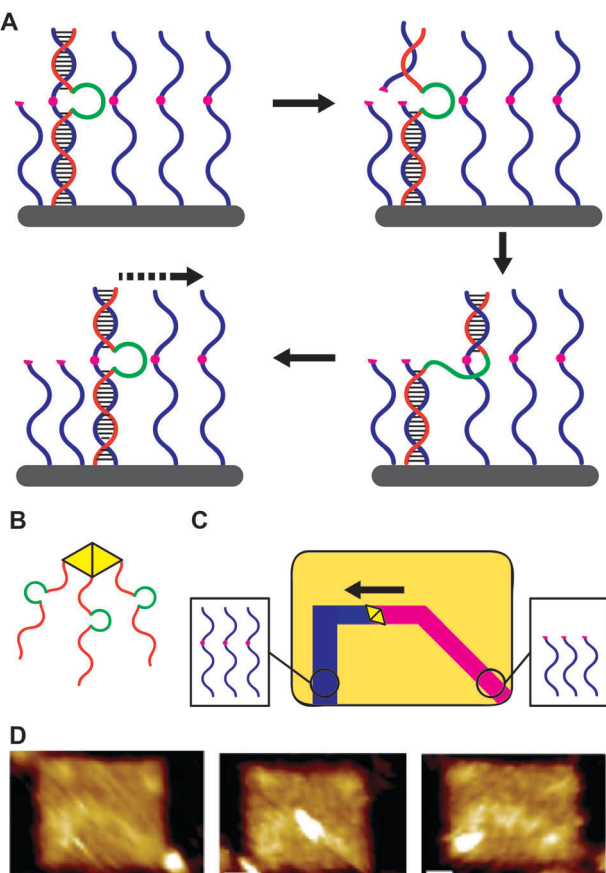


**Fig. 14** DNAzyme molecular walker. (A) Walker mechanism, where the DNA–aptamer sequence (green) that forms, in presence of magnesium, a DNAzyme capable of hydrolyzing the ribose base (pink dot) of the DNA-track. Subsequent release of the cleaved sequence leads to processive rebinding to the next strand and movement. (B) Multipedal DNAzyme spider and (C) its progress on a self-assembled prescriptive track of ribose-containing strands on a DNA tile. Blue tracks are the intact ones, pink are the consumed ones, and orange territory cannot be explored as it does not present track strands on its surface. (D) AFM images of the spider at the start, in the middle and at the end of the track (from left to right). Adapted with permission from (A) ref. 173 Copyright 2005, John Wiley and Sons, (B–D) ref. 175 Copyright 2010, Nature Publishing Group.

The first ones, internally fueled motors, consist of relatively large structures, which can be autonomous, but whose autonomy is limited by the amount of fuel they carry. The mechanisms rely on a localized conversion of fuel that pushes the object. Camphor boats are a classical example of propulsion.<sup>187</sup> In these systems, the camphor sublimes away from the solid scraps on the boat, adsorbs at the air/water interface, and locally lowers the surface tension of water close to the boat. The surface tension anisotropy around the boat generates a flow of water known as the Marangoni effect, which reciprocally pushes the boat towards camphor-free areas.<sup>188</sup> Surfactants present at the water surface can alter the motion,<sup>189</sup> and lead in some case to oscillatory movements.<sup>190</sup> Biocompatible motors with similar motion mechanisms have recently been demonstrated using a hydrophobic peptide fuel (surfactant) loaded in a metal organic framework and immobilized in a boat shape to foster directional movement.<sup>191</sup> These surface tension-driven mechanisms however restrict propulsion to interfaces.

To overcome interface-confined motors, colloidal-scale Janus particles consisting of an inert frame loaded with a water-reactive metal (*e.g.* gallium/aluminum alloy, magnesium or zinc) are an interesting alternative to propel in bulk solutions.<sup>192–194</sup> These systems are propelled by the reduction of water to hydrogen while the metal is oxidized. The asymmetric formation of hydrogen bubbles on the reducing metal side pushes the particles in the opposite direction (Fig. 15A and D). Such mechanisms enable propulsion in complex media, including for example blood serum,<sup>193</sup> but at the cost of reusability, since the motors are wasted once the metal is completely consumed.

Catalytic motors, the second class, benefit from being reusable, but they require a fuel-containing medium and can be sensitive to poisoning. Polymerization motors, inspired from actin assembly motors, propel objects by catalyzing the formation of rigid structures at one side (Fig. 15B). Suitable mechanisms to power the motion include the assembly of DNA hairpins at the edge of a DNA tile (Fig. 15E),<sup>195</sup> the polymerization of norbornene on one side of a Janus particle,<sup>196</sup> or the enzymatic production of a fibril-forming hydrogelator from a soluble precursor.<sup>197</sup>

Structure formation is not essential to motion, and, in fact, most of the catalytic motors only rely on an anisotropic distribution of the catalytic center creating an anisotropic chemical environment (Fig. 15C). Examples for such motors greatly vary in size and shape, from macroscale boats<sup>198</sup> to bimetallic nanorods,<sup>199–201</sup> Janus particles (Fig. 15F),<sup>202–204</sup> capsules,<sup>205</sup> tubes,<sup>206,207</sup> or polymersomes.<sup>208</sup>

The most common mechanism is the disproportionation of hydrogen peroxide, which creates bubbles, electrochemical proton flow or concentration gradients that propel the motors. For more details on their fabrication and motion mechanism a comprehensive review was recently published.<sup>209</sup>

A clear step towards propulsion mechanisms of higher biocompatibility is to replace the metallic catalysts by enzymes, which also opens up opportunities for enzyme-selective fuels. Several catalytic motors with immobilized enzymes showed propulsion in fluids by self-electrophoretic proton flow,<sup>210,211</sup> bubble

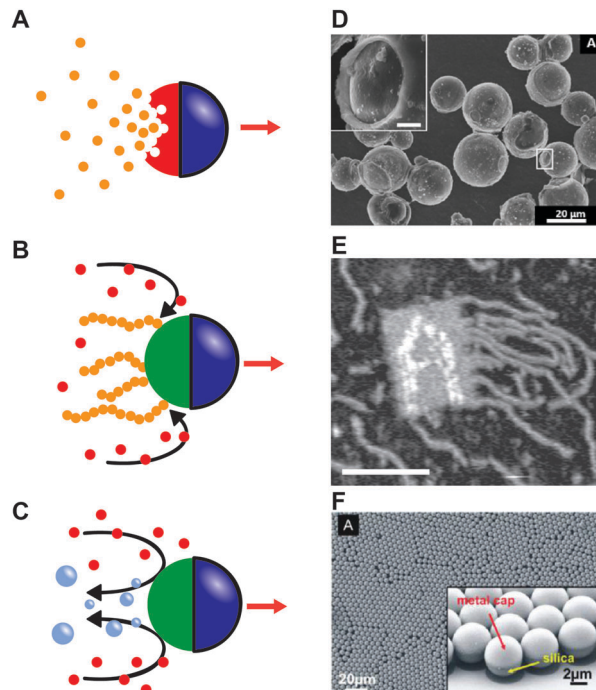


**Fig. 15** Self-propulsion of micro- and nanoscopic objects. (A) Internally fueled motor, in which the core reacts with water to propel the particle. (B) Polymerization motor and (C) catalytic motors featuring bubble propulsion. The fuel is in red and the catalytic areas are in green. The red arrows represent motions and the black arrow the flow of fuel. Examples of actual micromotors: (D) internally fueled, (E) DNA-based polymerization motor and (F) Janus catalytic motor. Adapted with permission from (D) ref. 193 Copyright 2013, John Wiley and Sons, (E) ref. 195 Copyright 2007, Nature Publishing Group, and (F) ref. 204 Copyright 2012, the American Chemical Society.

recoil,<sup>212,213</sup> or self-diffusophoresis<sup>214,215</sup> in the presence of the appropriate substrate. In fact, substrate-enhanced diffusion of enzymes alone has already been demonstrated for urease,<sup>216</sup> catalase,<sup>217</sup> RNA and DNA-polymerase,<sup>218–220</sup> even if the exact mechanisms of propulsion remain under debate.<sup>221,222</sup>

#### 4.4 Harnessing molecular work at the macroscale

The differences between the effect and principles of molecular switches and molecular motors on macroscale functionalities such as actuation or transport may not be obvious at first glance. There is no doubt that molecular switches can create macroscopic work, such as in the swelling/deswelling of hydrogels, movements of droplets on the surface with switched wettability or in the actuation of “artificial muscles” *e.g.* based on carbon nanotubes.<sup>223–225</sup> Certainly this has led to a range of fascinating responsive material concepts. The clear difference to the effect of molecular motors is the fact that returning to the initial state will undo/revert the work generated by triggering a previous switch. In contrast, a molecular motor can accumulate work by repetitive cycling.

One general challenge to create efficient macrostructures, no matter whether based on switches or motors, lies in the spatial organization of the individual molecular switches or motors. Disorganized systems waste molecular work because

individual movements may compensate each other. An important solution is to organize along a major director to accumulate movement in a single direction. For instance, crystals of light-responsive diarylethene are capable of changing shape and lifting weight upon irradiation.<sup>226,227</sup>

Such perfectly ordered macroscopic crystals are difficult to prepare, and hard to process or shape. Liquid crystals are known to combine long-range order with facile processing and alignment. The introduction of polymerizable groups also facilitates the fabrication of solid devices. In this respect, light-responsive liquid crystal elastomers are some of the most successful examples of molecularly organized systems for creating chemo-mechanical work (Fig. 16A).<sup>98,99,228–231</sup> Although these systems rely on switches rather than actual motors, they led to inspiring devices capable of walking,<sup>232</sup> swimming,<sup>233</sup> or pumping liquid<sup>234</sup> upon periodic irradiation (external actuation) and even rolling under constant and inhomogeneous irradiation.<sup>235</sup>

The organization of the molecular effectors impacts the function of the system. On the one hand, when the molecular switches work in parallel they generate high nominal forces capable of moving big objects, on the other hand, when the switches work in series they create movements of large amplitude.<sup>236,237</sup> For example, multiple light-powered molecular rotors working in parallel in a liquid crystalline film could rotate a rod 10 000 times their size.<sup>238</sup> In a different system similar rotors were used as crosslinkers in an organogel. Upon UV irradiation each rotor entangles the network at its proximity and the association in series of their individual motion results in the contraction of the organogel to 20% of its initial volume (Fig. 16B–D).<sup>239</sup> Note that the molecular motors make multiple transitions back to their original states, and accumulate work (volume change) continuously, which would not be possible for molecular switches. One of the ultimate goals is the assembly of muscle-like materials, in which the motors are polymerized in series and assembled in bundles to merge large amplitudes of motion and high forces.<sup>240</sup>

Another central challenge lies in the temporal organization and synchronization to promote long-lasting autonomous work generation, important for instance for pumping or walking, and similar to calcium signals that synchronize the myosin motors in muscles.<sup>146</sup> To this end, oscillating systems have proven to be a useful approach. For example pH oscillators (open reactors) can drive the rhythmic contraction or ciliary motion of pH-responsive polymers,<sup>241,242</sup> or the periodic bending of DNA-coated cantilevers,<sup>123</sup> and thus effectively convert chemical energy in mechanical work. However, since these systems do not store chemical energy they cannot operate in autonomy and stop functioning as soon as the reactant feeding stops.

So far the only systems generating mechanical work in autonomous chemical systems rely on the self-oscillating gels driven by the BZ reaction (see Sections 2.2 and 3.6).<sup>41</sup> The diffusion of feedback-controlling chemicals (bromine, bromous acid...) synchronizes swelling and contraction of the hydrogel, which leads to homogeneous oscillations in small gels.<sup>245</sup> However, as the size of the specimen increases, the characteristic diffusion times across the sample become larger than the period

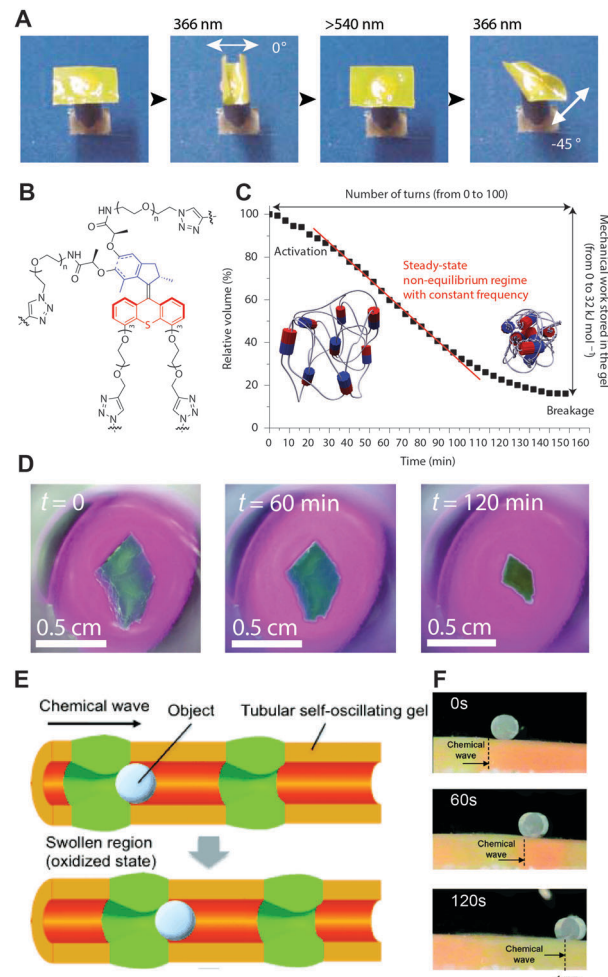


**Fig. 16** Macroscale devices capable of producing work. (A) A polymerized liquid-crystal film containing light responsive azobenzene switches. The film bends upon irradiation at 366 nm because the azobenzene isomerizations induce a longitudinal contraction of the liquid crystals. Irradiation above 540 nm flattens the film as the switches return to their initial conformation. Light polarization controls the bending direction by preferentially actuating crystal domains parallel to the polarization plane. (B) Chemical structure of the molecular motor crosslinking unit driving the contraction of a gel under UV light. (C) Schematic representation of the UV-induced entanglement together with the volume shrinkage of the corresponding gel. (D) Photographs of the gel at different times. (E) Schematic representation of peristaltic pumping with self-oscillating gels. (F) Photographs of an active surface transporting a small cylinder. Adapted with permission from (A) ref. 228 Copyright 2003, Nature Publishing Group, (B–D) ref. 239 Copyright 2015, Nature Publishing Group, (E) ref. 243 Copyright 2012, John Wiley and Sons and (F) ref. 244 Copyright 2009, the American Chemical Society.

of oscillation and different volumes of the same hydrogel simultaneously contract and swell. This leads to the appearance of complex patterns that depend (among other parameters) on the shape of the hydrogel.<sup>246,247</sup> A direct scale-up to large chemically powered devices is impossible because the loss of synchronization in large pieces prevents amplitude increase as swelling and deswelling in specific directions average out. It is possible to overcome this limitation by maintaining one dimension of the sample below the diffusion length of the chemicals. This has

led to self-oscillating hydrogel films showing propagating waves of swelling and contraction.<sup>248</sup> In such a case the local thickness increase (small dimension) is synchronous, while the width variations (large dimension) average out. This concept was applied to the fabrication of various functional devices, such as for the transport of small objects resting on oscillating surfaces (Fig. 16F),<sup>244,249,250</sup> the transport of bubbles, fluids and tracers in self-oscillating tubes (Fig. 16E),<sup>243,251</sup> as well as for the ciliary motion of microstructured surfaces.<sup>252</sup> It is important to note that while these systems can convert chemical energy into work autonomously, they do not violate thermodynamic laws since the work produced never exceeds the chemical energy consumed by the system.

Obviously further progress relies on a combination of temporal and structural synchronization. Key advances in this area deal with modifications of the internal structures of the BZ-hydrogels. A macroscopic structuring of the hydrogels with inhomogeneous crosslinking density can be used to design structures autonomously walking and swimming.<sup>253,254</sup> Furthermore, the integration of porosity allows drastically increasing the oscillation (swelling) amplitude,<sup>244,255</sup> while comb-type polymers with dangling responsive chains engineered on the molecular scale lead to faster and larger swelling/deswelling oscillations compared to conventional hydrogels.<sup>256,257</sup> These improvements aim at controlling the volume variation of the hydrogels during oscillations, and it is clear that more complex actuation principles and advanced operation will rely on combining the feedback mechanism for temporal synchronization with defined nano-/mesoscale organization of the molecular effectors for directional and most efficient chemo-mechanical energy conversion.

## 5. Information processing in autonomous systems

Chemical signals can modify the behavior of autonomous out-of-equilibrium systems, and can therefore provide them with the ability for sensing, adaptation and communication. Logic networks implemented in such systems are the key to allow for an appropriate adaptation in a complex sensory landscape with multiple signals. Improvements in the computational power of logic systems are needed to enable threshold sensing, signal filtering and even simple mathematic operations. Beyond simple adaptation, autonomous entities can also emit signals, and primitive forms of communication emerge when several autonomous entities adapt and exchange information simultaneously. Here it becomes obvious that a control over the emission rates and diffusion speeds of feedback-controlling chemical signals hold the key to modulate collective behavior and emergent properties.

### 5.1. Sensing, adaptation and communication in biology

Adaptation, the capacity to sense and respond to environmental variations, is crucial for the survival of living organisms. Even archaic unicellular organisms have developed complex molecular machinery to sense their environment and respond

to it. For instance, chemotaxis, the property of cells to move directionally in chemical gradients, allows them to find nutrients and escape from toxic environments.

Swimming prokaryotes such as *E. coli* (diameter  $\approx 2 \mu\text{m}$ ) alternate sequences of linear motion and random reorientation (tumbling; see Section 4.1 for more details). In order to direct themselves in a chemical gradient, the bacteria change their tumbling frequency according to the concentrations of target chemicals. For instance, *E. coli* possesses several trans-membrane histidine–aspartate phosphorelay systems that sense the presence of chemo-attractants (pH, nutrients, oxygen level...) in the environment, and exert, through phosphorylation signals, a negative feedback on the frequency of the clockwise rotation of the F1-ATPsynthase rotor. The decrease of the clockwise rotation frequency reduces chaotic tumbling and increases the lengths of linear motion sequences. This causes the bacteria to move faster as the chemo-attractant concentration increases, promoting motion towards concentrated areas (Fig. 17A). Similar regulating systems sensitive to chemo-repellants that increase the tumbling frequency allow the bacteria to move away from such signals.<sup>258,259</sup>

Larger eukaryote organisms such as *Dictyostelium* ( $10 \mu\text{m}$ ) can directly sense chemical gradients due to their larger size (Fig. 17B). A chemo-attractant (e.g. cyclic adenosine monophosphate) is detected by trans-membrane receptors that induce a matching gradient of G-proteins in the cytoplasm. A locally excitable and globally inhibited (LEGI) regulatory network amplifies this gradient and generates a sharp, thresholded signal at the front of the bacteria. Shortly, the LEGI network consists of an activator (positive feedback), which degrades quickly, combined with an inhibitor with a longer lifetime (negative feedback). Because of its slow degradation the inhibitor diffuses in the entire cell and the negative feedback applies everywhere proportionally to the average level of the chemo-attractant. This erases the average background concentration. In contrast, the short lifetime of the activator causes the positive feedback to overcome inhibition only at the gradient front (Fig. 17C and D).<sup>260–263</sup> Actin polymerization and the appearance of pseudopodia responsible for cell migration follow the signal front and initiate motion towards areas of high concentrations of the chemo-attractant.

Importantly, there are common mechanisms for adaptation in these two chemotaxis processes for both prokaryotes and eukaryotes: they both consist of a sensing system coupled to a logic network (of different complexity) that finally regulates the function (here the motion mechanism).

Colonies of bacteria push adaptation to the next hierarchical level. Each organism emits chemical signals to communicate with the colony. Thereby they can monitor the population density in the colony and adapt their behavior accordingly – a feature called quorum sensing. *Vibrio fischeri* for example, a marine bacterium, emits bioluminescence only at high population density. This behavior, based on quorum sensing, evolved in symbiosis with a squid that uses the bioluminescence of these bacterial colonies to confuse predators. Crowd induced bioluminescence therefore increases the survival of

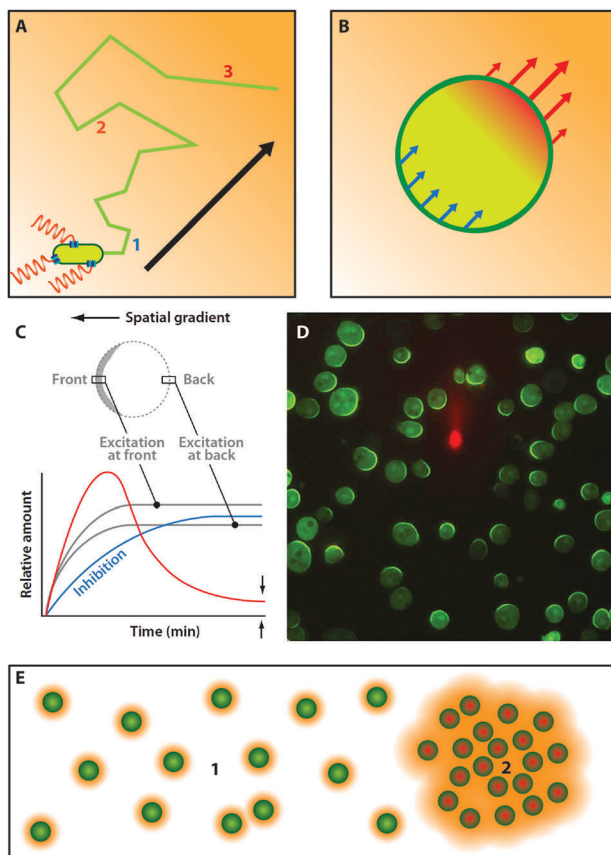


**Fig. 17** Examples of biological adaptation on different levels. (A) Chemo-taxis of flagellar bacteria. As the chemo-attractant increases (orange background) the frequency of tumbling decreases and allows larger linear moves into the direction of the chemo-attractant. (B) Chemo-taxis of eukaryotes. A logic network transfers the gradient of chemo-attractant into a thresholded signal gradient and regulates actin polymerization at the origin of motion. (C) Response of the Locally Excited Globally Inhibited (LEGI) network to the gradient of chemo-attractant. Grey lines: local excitation. Blue line: inhibition feedback to allow for threshold sensing between front and back. Red line: net signal response at the gradient front (excitation minus inhibition). (D) Response of immobilized *Dictyostelium discoideum* in a gradient of cyclic AMP provided by a micropipette labeled in red in the center. The signaling proteins of the cells are fused with a green fluorescent protein. The green crescent fluorescence oriented to the center are representative of the gradient sensing of the cells. (E) Schematic representation of quorum sensing. As the local cell density increases from (1) to (2) the cells switch behavior, increase the emission of signaling molecules, and create a new functional output (e.g. bioluminescence). Adapted with permission from (C) ref. 260 Copyright 2010, the National Academy of Science and (D) ref. 263 Copyright 2004, Nature Publishing Group.

both the squid and the colony while isolated bacteria save energy by switching the light off (Fig. 17E).<sup>264–266</sup>

Other chemical signals and logic networks controlling communication among unicellular organisms enable collective hunting,<sup>267,268</sup> self-organization in complex fruiting bodies,<sup>269</sup> maze solving,<sup>270</sup> and the creation of robust colony networks.<sup>271</sup>

Highest complexity is of course encountered in multicellular organisms, in which the continuous exchange of interacting chemical signals drives the formation of complex shapes and multifunctional organs from a spherical unicellular zygote.

This spontaneous formation of shapes from an out-of-equilibrium chemical system is called morphogenesis. In 1952, Turing described in mathematical terms how two hypothetical chemical morphogens diffusing and interacting with each other could spontaneously form patterns from an initially homogeneous medium.<sup>272</sup> While the molecular nature of the morphogens at the origin of most biological patterns and shapes remains unknown, the model became popular to describe and explain pattern formation in living organisms.<sup>273,274</sup> Recreating Turing patterns *in vitro* helps to understand biological morphogenesis and can drive the fabrication of new intelligent systems.

## 5.2. Artificial chemotaxis

Many catalytic nano- and micromotors (Section 4.4) show an apparent diffusion coefficient positively correlated with the concentration of chemical fuels in their environment (Fig. 18A).

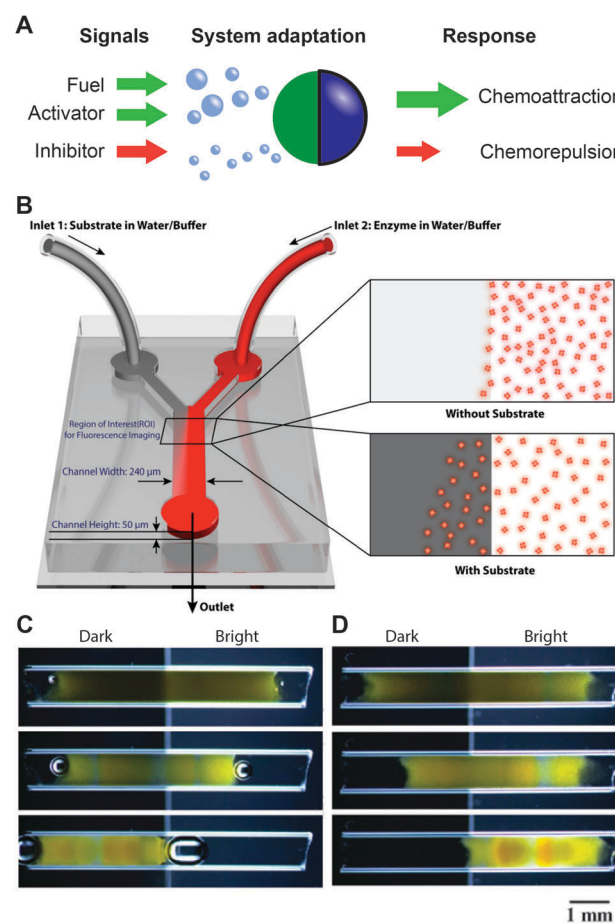


**Fig. 18** Artificial chemotaxis. (A) Schematic representation of possible signal-induced nano-/micromotor responses. (B) Chemotaxis of enzymes towards areas of high substrate concentration in a microfluidic device. (C and D) Phototactic motion of a self-oscillating BZ gel under anisotropic illumination in a glass capillary top at  $t = 0$  min down at  $t > 150$  min. (C) The gel is phototropic under low illumination (dark area  $33 \mu\text{W cm}^{-2}$ , bright area  $106 \mu\text{W cm}^{-2}$ ) and (D) photophobic under high illumination (dark area  $205 \mu\text{W cm}^{-2}$ , bright area  $904 \mu\text{W cm}^{-2}$ ). Adapted with permission from (B) ref. 217 Copyright 2013, the American Chemical Society and (C and D) ref. 286 Copyright 2013, the Royal Society of Chemistry.

In the presence of a fuel gradient they move towards areas of high fuel concentration with a mechanism resembling the chemotaxis of *E. coli* (Fig. 18A). This behavior has been reported for instance for enzyme-powered micromotors,<sup>214</sup> polymerization motors,<sup>196</sup> bimetallic rods,<sup>275</sup> and stomatocyte-like motors.<sup>276</sup> It is the simplest form of chemotaxis as the signal is also the fuel of the motor. Interestingly enough, substrate-induced chemotaxis was also reported for pure enzymes,<sup>217–219,277</sup> and applied to the separation of mixtures of enzymes in microfluidic devices (Fig. 18B).<sup>277</sup> The overall simplicity of fuel-driven chemotaxis limits the adaptability because nano-/micromotors can only direct themselves in fuel gradients.

Efforts to direct the motion of nano-/micromotors with signals other than fuel gradients focus mainly on external magnetic fields, for which there is however no underlying molecular mechanism.<sup>278–280</sup> Additional possibilities arise to direct catalytic nano-/micromotors fueled by hydrogen peroxide using pH, which influences the rate at which the fuel is being consumed.<sup>281</sup> Such pH-induced chemotaxis was also reported for internally fueled motors based on peptide reorganization,<sup>282</sup> and surfactant-induced propulsion.<sup>283</sup> Further opportunities arise for new chemotaxis mechanisms, using *e.g.* catalytic inhibitors to induce chemophobic motion (away from chemo-repellant),<sup>284</sup> or light-activated catalysts to implement phototropic behavior (towards light).<sup>285</sup>

Towards light-modulated behavior, it is interesting to point to autonomously self-oscillating BZ hydrogels, which contain a photo-sensitive ruthenium catalyst rendering their oscillations light-dependent (Sections 3.6 and 4.4).<sup>244,253,254,287,288</sup> Phototactic self-oscillating hydrogels were initially proposed in computer simulations.<sup>289,290</sup> Recent experiments on BZ gels could show that, depending on the light intensity, the gel can either be tweaked to be phototropic (low light intensity) or photophobic (high light intensity; Fig. 18C).<sup>286</sup>

A more sophisticated signal-induced chemotaxis can be implemented in molecular systems based on DNA walkers powered by a nicking enzyme. The system consists of a network of tracks assembled on a DNA tile where each track can be selectively activated by strand displacement reactions. Based upon this principle, the addition of single-strand signals to the medium allows controlling the final destination of the walker.<sup>182</sup>

All of these examples remain relatively simple as the signals directly regulate the activity driving the motion. Systems capable of choosing their direction from multiple and competitive signals will be a future milestone, but this requires an intermediate logic mechanism that treats the signals and regulates the response.

### 5.3. Implementing intelligence with logic networks

Living organisms use logic networks and computing systems to couple their adaptive structures (microtubules, kinesin motors...) to their sensory systems. This is necessary to navigate in a complex sensory landscape with multiple signal inputs.<sup>291</sup> It allows for example *E. coli* to move simultaneously away from chemo-repellents and towards chemo-attractants.

The possibility to encode Boolean logic operations in various chemical reactions has gained in popularity in the last decade.

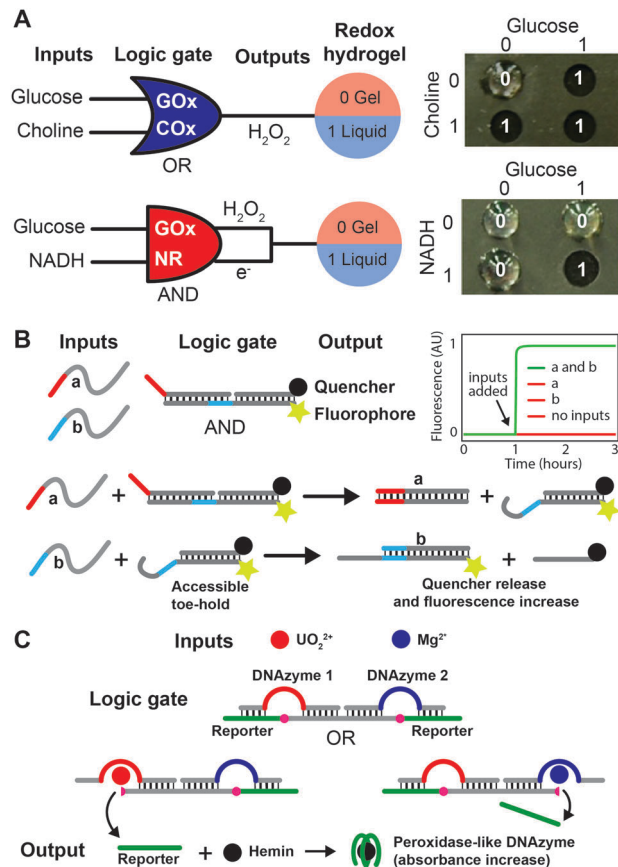


**Fig. 19** Logic operations in various molecular systems. (A) Logic gates implemented from enzymatic reactions. The OR gate contains glucose oxidase (GOx) and choline oxidase (COx). Either glucose or choline leads to the production of  $\text{H}_2\text{O}_2$ , which induces the dissolution of the responsive hydrogel. The AND gate contains glucose oxidase (GOx) and nitroreductase (NR) and two supramolecular hydrogel networks, one dissolving in presence of  $\text{H}_2\text{O}_2$  and the other dissolving in presence of  $\text{e}^-$ . Both NADH and glucose are required to trigger the hydrogel dissolution. (B) A strand displacement AND gate, in which the addition of the two inputs (strands a and b) releases the quencher bound oligomer from the duplex (output) and induces a fluorescence increase. If input a is missing there is no toe-hold accessible for b to displace the quencher strand, if b is missing the quencher and the fluorescent oligomer remain hybridized and the fluorescence remains negligible. (C) A DNAzyme OR logic gate that senses metal ions. Each DNAzyme releases the same reporter DNA strand in presence of the correct input ( $\text{Mg}^{2+}$  or  $\text{UO}_2^{2+}$ ). The output reporter strand complexes a hemin and forms a peroxidase-mimicking DNAzyme. Adapted with permission from (A) ref. 304 Copyright 2014, Nature Publishing Group, (B) ref. 66 Copyright 2006, the AAAS and (C) ref. 307 Copyright 2009, the American Chemical Society.

Responsiveness based on molecular logic has been implemented based on a wide diversity of substrates, ranging from small organic molecules<sup>292–294</sup> to enzymes,<sup>295,296</sup> DNA or DNAzymes (Fig. 19).<sup>66,297,298</sup>

In this section, we will first discuss the construction of simple logic gates with a focus on the nature of their input and output because they determine the complexity of the sensory landscape and the diversity of adaptations accessible. Later, we will discuss different approaches to increase the complexity of logic controllers towards the design of intelligent systems.

Most chemical reactions can be understood as logic gates. For example glucose oxidase is an enzyme that converts glucose in gluconic acid in the presence of oxygen. It can therefore be viewed as an AND gate, meaning that gluconic acid (Output) forms only when glucose (Input 1) and oxygen (Input 2) are present. Similarly, an enzyme capable of catalyzing the conversion of two substrates indifferently can be viewed as an OR gate. In fact most basic logic gates (AND, OR, XOR, NOR...) have been implemented with enzymatic reactions.<sup>299,300</sup>

Such enzyme outputs (products) can be used to trigger and actuate suitable responsive materials. Logic gates operated by enzymes and generating a pH variation were for example coupled to bio-fuel cells,<sup>301</sup> hydrogel membranes,<sup>302</sup> or pH-responsive nanoparticles.<sup>303</sup> Fig. 19A demonstrates one exemplary system, in which a combination of enzymes is used to create OR and AND gates to regulate the disassembly of specifically designed redox-sensitive peptide hydrogels.<sup>304</sup> The OR enzymatic gate uses two enzymes, choline oxidase (COx) and glucose oxidase (GOx), that independently release H<sub>2</sub>O<sub>2</sub> in the presence of their respective substrates. These enzymes are embedded in a H<sub>2</sub>O<sub>2</sub>-sensitive supramolecular peptide network; the hydrogel therefore dissolves (response) in the presence of either glucose or choline (inputs) due to their enzymatic conversion into H<sub>2</sub>O<sub>2</sub> (output). Similarly, the AND enzymatic gate consists of two enzymes, glucose oxidase (GOx) and nitroreductase (NR) embedded in a double supramolecular network gel, one dissolving in the presence of H<sub>2</sub>O<sub>2</sub> and one dissolving in the presence of e<sup>-</sup> (*i.e.* nitroreductase transfers electrons from NADH to the nitro group of the hydrogelator). Such a hydrogel therefore dissolves when both networks disappear, that is when both glucose and NADH are present (each input, respectively, corresponds to the GOx and NR substrates). This system provides an inspiring proof of principle design for logic-gated hydrogel dissolution conditioned to the presence of biological signals.

In the DNA world, the implementation of logic circuits and advanced computation modules relies largely on strand displacement reactions and DNAzymes. A simple example of a strand displacement logic gate is presented in Fig. 19B. The construct uses the DNA oligomers a and b as inputs and releases a quencher bound oligomer as output. The system allows easy fluorescence readout as physical separation of the fluorophore and quencher decreases the FRET efficiency (Förster Resonance Energy Transfer). The mechanism is the following: the strand a binds to the red toe-hold and displaces its complementary strand to form an inert duplex. Thereby it reveals the blue toe-hold necessary for strand b to start the next displacement reaction, resulting in the release of the quencher bound oligomer. In the absence of strand a the blue toe-hold remains in its inactive duplex form and strand b cannot bind to the gate to release the quencher. The construct therefore functions as an AND gate (*i.e.* a and b are needed for fluorescence increase).<sup>66</sup> Indeed the output single-stranded oligomer can be used as input for another gate allowing construction of complex networks as discussed further below.

DNAzymes, *i.e.* DNA sequences that catalyze specific reactions (RNA hydrolysis or DNA ligation for example), can also serve as

logic gates.<sup>305</sup> In such systems the inputs modify the shape of the active site of the DNAzyme and activate or inactivate its catalytic activity. For instance the OR gate presented in Fig. 19C consists of two DNAzymes which respectively require uranyl and magnesium ions to hydrolyze the RNA base (pink dot) of the construct. Because after hydrolysis each DNAzyme releases the same reporter strand both uranyl or magnesium lead to a positive output (formation of a new peroxidase mimicking DNAzyme). This OR gate also illustrates the versatility of DNAzymes as interfaces to sense pH,<sup>306</sup> metal ions,<sup>307,308</sup> adenosine monophosphate or cocaine inputs,<sup>309</sup> in addition to the traditional DNA signals.<sup>310,311</sup>

A beautiful example of a functional logic gated device was reported recently. The system consisted of a DNA origami capsule closed by two DNA aptamers (sequences similar to the ones of DNAzymes that change shape upon binding with their targets). The capsule functions as an AND gate and opens only in the presence of both target antigens, allowing it to release its cargo. The carrier can therefore recognize target cells in mixtures of cell and in whole blood samples.<sup>312</sup> Such passive devices are an interesting milestone towards intelligent materials that sense signals with high selectivity from a complex environment.

Increasing the level of “intelligence” of materials controlled by logic operations requires building complex networks beyond single logic gates. Boolean formalism (a language built for binary logic) facilitates the construction of such computing networks. To this end, there have been approaches using enzymatic cascades, where the product of one enzyme serves as a substrate of the next one, which allows connecting several gates to perform a more complex task. Networks able to code basic arithmetic operations such as the half-adder and half-subtractor, or padlocks (concatenated AND gates) were for example built using classical enzymes and substrates.<sup>313,314</sup> However, the versatility and complexity of such enzyme networks remain limited, because each new step requires the integration of a new enzyme compatible with the entire system. This ultimately faces limitations as multiple enzymes may interfere with each other and cannot work independently in a highly complex system.

While appropriate compartmentalization may provide a solution, this problem can be overcome by going to DNA-based systems, where multiple entities can interact in parallel and with high selectivity. This allows for the design of intelligent systems of much higher complexity and functionality. In addition to classic arithmetic operations,<sup>315,316</sup> several DNAzyme automata capable of playing TIC-TAC-TOE were built.<sup>317,318</sup> More recently multi-layered logic circuits,<sup>319</sup> versatile modular libraries,<sup>311</sup> and programmable automata<sup>320</sup> were also reported.

Nonetheless, even with DNA logic it is difficult to increase the number of reaction cascades beyond a few levels because leaking and non-quantitative operations lead to a poor signal-to-noise ratio. Such problems can however be compensated when going to analogic gates (non-Boolean logic systems) that adjust the amplitude of the signal, for example by thresholding or amplifying it.<sup>66,321,322</sup> This drastically reduces the noise,

and allows us to build more complex circuits, yet at the expense of the speed of computation.

Success in this direction enabled to build one of the most complex logic circuits so far, that is able to calculate the square root of a four bite number (*i.e.* From 0 (0000) to 15 (1111)) by strand displacement reactions based on a network of 130 individual DNA strands (Fig. 20A).<sup>323</sup> For the calculation, the decimal number is converted into its four bit binary equivalent. Each bit of the binary number corresponds to the addition of input strands from  $X_1$  to  $X_4$ . The system is based on a dual-rail logic meaning that there is a signal strand coding for “0” and a signal strand coding for “1”. For instance, the decimal number “1” is written as “0001” in binary, meaning that the inputs “0” are introduced for  $X_4$ ,  $X_3$  and  $X_2$  while input “1” is introduced for  $X_1$ . Strand displacement reactions encoded in partially hybridized duplexes, and fueled by single-stranded oligomers are then used to process these inputs. Each Boolean logic gate (signal processing) is combined to an analogic threshold gate (noise reduction) and amplification gate (signal restoration) allowing efficient multilevel concatenation. At the end, the network can displace four different fluorophore–quencher duplexes (similar to the one in Fig. 19B) leading to four possible fluorescent readouts, respectively, coding for  $Y_2 = 0$ ,  $Y_2 = 1$ ,

$Y_1 = 0$  and  $Y_1 = 1$ . The result is a two bit number  $Y_2Y_1$  equal to the integer part of the square root of the input, and which can be converted back to the decimal equivalent (*i.e.* from 00 for 0 to 11 for 3). Examples of decimal and binary input and output are presented in Fig. 20B and C.

This example highlights one of the conceptual differences between building computational/logic networks based on chemical species as opposed to classical electronics. Since chemical reactions or supramolecular hybridization are still far from being 100% selective and achieving 100% conversion, it may well be that binary language (that supports all silicon electronics) may not naturally suit logic implementation with chemical systems.

In contrast, neural networks inspired by the brain rely on analogic signal treatment and adapt more naturally to chemical logic.<sup>325</sup> For instance a consensus network capable of comparing the intensity of two inputs and converting the minority signal into the majority one is relatively easy to implement with strand displacement reactions (Fig. 20D), while it would be harder with binary logic.<sup>324</sup> Interestingly, such selection strategies (from minor to major) are also relevant with respect to (directed) evolution of chemical species in complex fitness landscapes – a topic deeply relevant to systems chemistry and origin-of-life research.

Towards a simplification of complex DNA networks, it is important to point to further advantages provided by enzymatic replication of DNA templates (*cf.* Section 2.4).<sup>57</sup> Without going into details, those can streamline the implementation of complex logic tasks.<sup>326–328</sup> For example, the construction of a neural network coding for a four neuron associative memory only requires 16 template strands and 3 enzymes<sup>329</sup> compared to 112 strands for a similar network solely based on strand displacements.<sup>325</sup>

#### 5.4. Communication and collective behavior of systems with discrete entities

Discrete entities in groups of out-of-equilibrium systems can emit and sense molecular signals across a passive medium. Unique collective behavior emerges from this primitive form of communication (Fig. 21A). For example catalytic nano-/micromotors generate chemical gradients around them as they consume fuel, and we have seen in Section 5.2 that they can also sense such gradients. If the chemical gradients created around each nano-/micromotor provide sufficient attractive, phoretic force, the self-propelling objects will swarm to form dynamic clusters, which spontaneously re-disperse when the fuel runs out.

Swarming has for example been reported for catalytic Au particles in a solution containing both hydrazine and hydrogen peroxide,<sup>330</sup> or for Janus catalytic motors solely fueled by hydrazine.<sup>331</sup> Internally fueled UV-driven AgCl micromotors also undergo swarming.<sup>332</sup>

If the gradient created around the motor particles is repulsive, the particles will avoid each other. This even allows switching from attractive swarming to repulsion. To this end, it has been shown that the addition of ammonia to internally fueled  $\text{Ag}_3\text{PO}_4$  micromotors inverts the direction in which the particles move in the gradient created by other particles. Ammonia thus acts as an

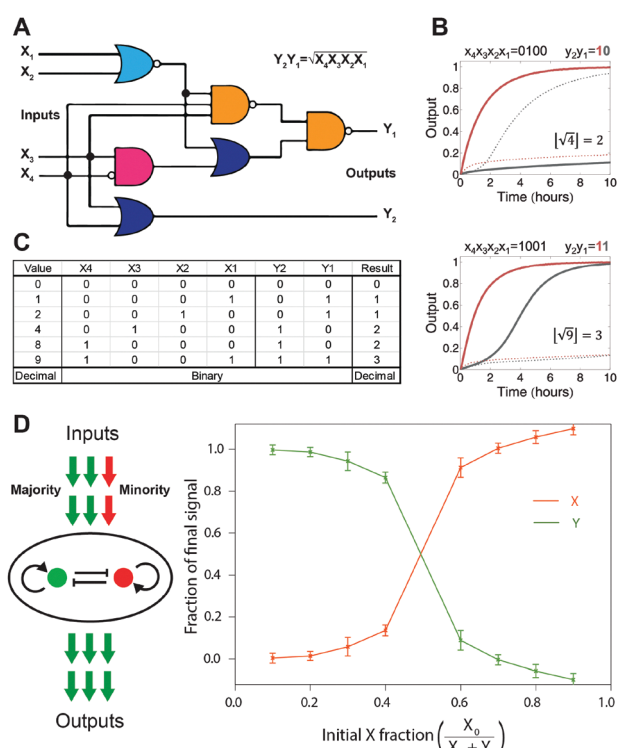


Fig. 20 Complex logic networks able to perform computations and signal processing. (A) Network of concatenated DNA logic gates calculating the square root of a four bit number. (B) Examples of fluorescent outputs for the input values 4 and 9. (C) Table showing the conversion of few decimal numbers, into 4 bit binary inputs ( $X_4X_3X_2X_1$ ), the corresponding output ( $Y_2Y_1$ ) and the decimal result. (D) A strand displacement network that compares two inputs and generates as output the major input. Adapted with permission from (A–C) ref. 323 Copyright 2011, the AAAS and (D) ref. 324 Copyright 2006, Nature Publishing Group.

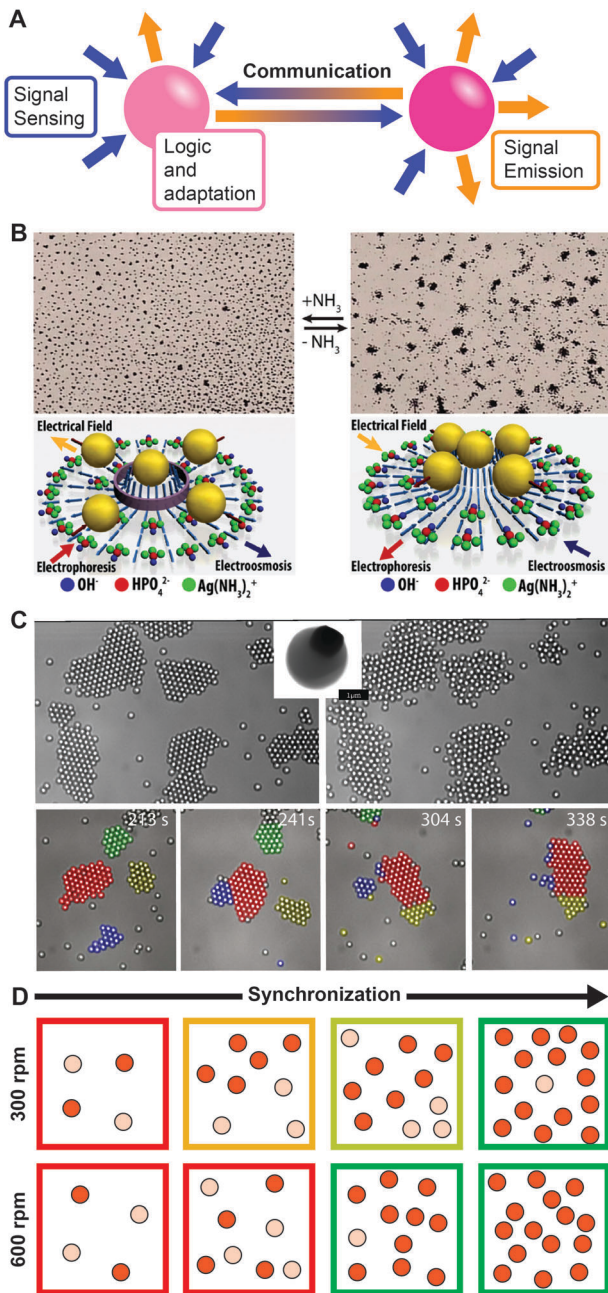


Fig. 21 Communication and collective behavior of systems with discrete entities. (A) Schematic representation of communication between two out-of-equilibrium entities. (B) Dispersions of  $\text{Ag}_3\text{PO}_4$  particles switching from swarming to self-avoidance. Upon addition of ammonia the gradient created by each particle turns from chemo-attractive to chemo-repellant for its neighbors. (C) (left) "Living" crystals formed upon irradiation of the Janus micromotors (TEM inset scale bar 1  $\mu\text{m}$ ). (right) Crystal dissolution 10 seconds after the light is switched off. (bottom) Dynamic crystal rearrangement, the false colors show the time evolution of particles belonging to different clusters. (D) Schematic representation of progressive (up, slow stirring rate) and abrupt (down, fast stirring rate) synchronization of oscillating particles with increasing population density. Adapted with permission from (B) ref. 333 Copyright 2013, the American Chemical Society, (C) ref. 335 Copyright 2013, the AAAS and (D) ref. 337 Copyright 2009, the AAAS.

external logic control that modifies the collective behavior of the micromotors from swarming to self-avoidance (Fig. 21B).<sup>333</sup>

Competition between attractive and repulsive forces can also drive more complex behaviors.<sup>334</sup> A striking example deals with monodisperse Janus motors that form two-dimensional, highly dynamic ("living") crystals upon UV-triggered propulsion.<sup>335</sup> The large crystals spontaneously break and reform due to the competition between attraction (phoretic and osmotic) and self-propulsion that pulls the colloids apart (Fig. 21C). In the presence of hydrogen peroxide  $\text{AgCl}$  micromotors also autonomously alternate between fast disorganized motion and aggregation.<sup>336</sup>

New collective behavior emerges when the particles themselves are the ground of a feedback-regulated molecular network. For instance, populations of compartmentalized oscillatory reactions in hydrogel beads can communicate through the exchange of inhibitors and activator intermediates (controlling the feedback mechanisms) across passive media.<sup>338</sup> In such a system, the exchange of information is driven by diffusion and hence depends on the shape,<sup>339</sup> the packing geometry,<sup>340</sup> the catalyst loading,<sup>341</sup> and the active substrates. Strikingly, it is possible to observe a primitive form of quorum sensing in such a system. Large populations of oscillating particles switch from independent to synchronized behavior as the particle density increases (Fig. 21D).<sup>337</sup> The stirring rate of the particle suspension, which relates to the distance at which the particles communicate (average distance covered by the activator and the inhibitor), controls the nature of the transition. Slow stirring induces a gradual transition, while fast stirring promotes a sudden synchronization.

Because of their complex dynamic nature oscillatory reactions could lead to more elaborate behavior. Theoretical models foresee the creation of capsule colonies that follow each other,<sup>342</sup> cilia that synchronize their oscillations,<sup>343</sup> or macroscopically oscillating gels that spontaneously self-organize.<sup>344,345</sup>

### 5.5. Emergent behavior from reaction-diffusion in continuous systems

In out-of-equilibrium chemical systems where diffusion and mixing are slower than the reactive process, the local chemical state may change across the material. We encountered such systems already for self-oscillating hydrogels discussed in Section 4.4. Each infinitesimal sub-element of the material therefore exchanges chemical information with its neighbor by diffusion (communication) while local, feedback-controlled reactions take place (Fig. 22A).

New properties emerge from such continuous reaction-diffusion systems, in which the material adapts to its environment both spatially and temporally. They can support long-range signal transport, spatial sensing or lead to the spontaneous appearance of patterns.

Primitive mechanisms for signal transport are the easiest to build as self-accelerating reactions (positive feedback) lead to the appearance of propagating fronts of chemical potential. For example, a system presenting a single positive feedback mechanism such as the urea/urease reaction discussed in Section 2.3 can support long-range signal transport (Fig. 22B).<sup>346</sup> The mechanism is the following: urea and urease are mixed under acidic conditions and cannot react as the enzyme is inactive. Subsequently, a local addition of base (signal) activates the urease,

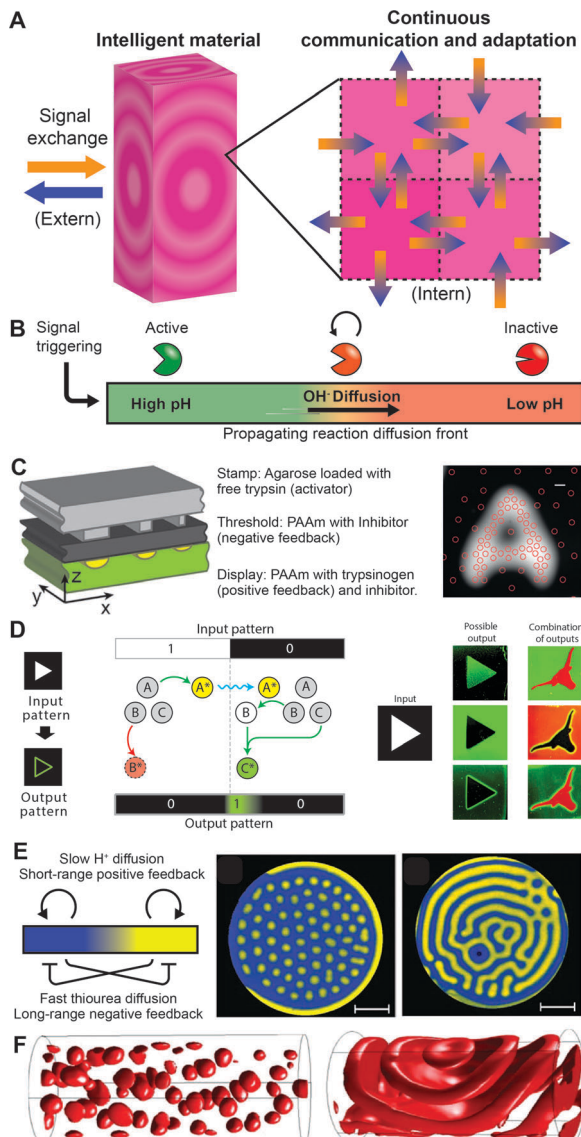


**Fig. 22** Reaction-diffusion systems in continuous materials. (A) Schematic representation of the infinitesimal unit cell communicating through diffusion in an intelligent out-of-equilibrium material. (B) Enzymatic propagation of a pH reaction-diffusion front with positive feedback. (C) Spatial sensing device for trypsin. The stamp (light grey top) contains trypsin, the network activator. In the threshold layer (dark grey middle) the inhibitor erases low trypsin concentrations. The display layer (green down) contains the full autocatalytic reaction network and generates a localized fluorescent signal in the presence of trypsin. (right) Actual example of output (bright area) and stamp contact point (red circle), fluorescence appears only when the density of contact points overcome the threshold level. (D) (left) Network of strand displacement reactions leading to edge recognition. UV simultaneously activates A and deactivates B; the fluorescent probe C is only activated near the edge where A\* and B can react by diffusion. (right) Examples of outputs with one and two display reaction networks. (E) Schematic representation of the short-range positive feedback and long-range negative feedback leading to the appearance of 2D Turing patterns in one-side-fed unstirred reactor with thiourea–iodate–sulfite reaction (scale bar 4 mm). (F) Topographically reconstructed concentration fields for 3D Turing patterns obtained in capillary with a diameter of 0.6 mm. Adapted with permission from (C) ref. 348 Copyright 2014, John Wiley and Sons, (D) ref. 349 Copyright 2013, Nature Publishing Group, (E) ref. 350 Copyright 2009, the AAAS, and (F) ref. 351 Copyright 2011, the AAAS.

which starts converting urea into ammonia increasing further the pH. The diffusion of ammonia then neutralizes the acid and activates nearby enzymes. The process leads to the propagation of a pH wave from the trigger point across the entire system. The main advantages of using an autocatalytic pH feedback system for signal propagation as opposed to simple diffusion of the trigger signal (base droplet) are trigger amplification, maintained signal intensity over long distances and higher propagation speeds. Similar pH waves, with an opposed transition from high to low pH, were also observed based on the autocatalytic (positive feedback) oxidation of glucose by glucose oxidase.<sup>347</sup>

In order to promote spatial sensing, it is necessary to confine the signal amplification driven by the autocatalytic process by a negative feedback preventing propagation away from the signal point. Sensing devices were for example built using the components of the trypsin oscillator discussed in Section 2.3. When the trypsinogen substrate and the inhibitor are embedded in a single hydrogel layer, the device is capable of reporting the spatial distribution of trypsin by simple contact with high sensitivity.<sup>352</sup> Trypsin diffusion locally triggers the autocatalytic conversion of trypsinogen, which leads to the amplification of the signal while the inhibitor, which reversibly binds to trypsin and impedes the catalytic activity, prevents long-range amplification ensuring high spatial resolution. A separation of the inhibitor and the substrate in a bi-layer promotes threshold sensing, where only high local concentrations of trypsin (that overcome the inhibitor concentration in the first layer) are reported (Fig. 22C).<sup>348</sup>

Towards a more advanced sensory system, light-triggered uncaging of single-stranded DNA combined with strand displacement logic opens up opportunities to create intelligent photo-sensing hydrogels.<sup>349</sup> Similar to classical photo-responsive systems, it is possible to create positive and negative replicates of the pattern, because light either triggers or inhibits the response. However, the system can also recognize the edges of the pattern due to selective reactions at the interface of irradiated and non-irradiated areas. The mechanism relies on two DNA modules, where one is activated ( $A \rightarrow A^*$ ) while the other is de-activated ( $B \rightarrow B^*$ ) by light (Fig. 22D). At the edge, the light activated module ( $A^*$ ) can diffuse and react with its counterpart (B) that remained active in the unexposed region, generating the fluorescent output ( $C \rightarrow C^*$ ). Two orthogonal DNA reaction networks combined inside such a hydrogel can simultaneously report arbitrary combinations of outputs from the same input pattern.

The diffusion speeds of the chemical signals driving the feedback mechanisms in oscillatory systems define the distance at which sub-elements communicate with each other. Therefore, controlling the diffusion speed of each feedback-regulating species facilitates the emergence of new behavior. Control over the diffusion speeds can be achieved by compartmentalization, selective solubilities of signaling chemicals, or by complexation of such signals with compounds of low diffusivity.

For example, unstirred inorganic oscillating reactions are known to present propagating waves of chemical potential (signal transport),<sup>22,353–356</sup> and photosensitive catalysts were used to create

devices that memorize and process images (spatial sensing).<sup>39,357</sup> Running such reactions in water-in-oil microemulsions allows some control over the diffusion speeds of the interacting chemicals of the BZ systems. Since polar molecules (*e.g.* Br<sup>-</sup>) remain trapped in the water droplets (slow diffusion) while apolar ones (*e.g.* Br<sub>2</sub>) can cross the continuous oil phase (fast diffusion), it is therefore possible to adjust internal communication by choosing the volume fraction of oil in the system. Note that this system is significantly different from the quorum sensing one described in Section 5.4 since individual compartments are too small and dissimilar to be considered individually (many do not even contain a catalytic unit).<sup>358</sup> Based on this concept a photosensitive recording device was constructed, whose memory time lasted for hours,<sup>359</sup> and new spatial patterns such as segmented waves,<sup>360</sup> inwardly rotating spirals,<sup>361</sup> as well as standing Turing structures were reported.<sup>358,362,363</sup> One of the most impressive demonstrations with this microemulsion system probably consisted in the first observation of 3D chemical Turing patterns (Fig. 22F).<sup>351</sup>

The engineering of diffusion speeds and communication timescales in oscillating bulk systems can further be addressed by selective complexation with compounds altering the diffusion rates of feedback-regulating chemicals (Fig. 22E).<sup>350,364</sup> For instance, a low mobility complexation agent (poly(sodium acrylate)) was introduced into the oscillatory thiourea-iodate-sulfite system to selectively reduce the diffusion speed of the proton serving as the positive feedback signal. The control of diffusion speed between the activator (proton) and the inhibitor (thiourea) led to the first rational implementation of Turing patterns in unstirred open reactors.<sup>350</sup>

An excursion into the DNA world shows that versatile approaches to engineer complex patterns are on the way of being developed. Enzymatic replication of DNA templates (discussed Sections 2.4 and 5.3) and their assembly in reaction networks already showed oscillatory behavior in closed systems,<sup>57</sup> and propagating fronts in unstirred reactors.<sup>365</sup> A recent work also showed that it is possible to tune the diffusion speed of the interacting chemicals using surfactant bound DNA oligomers.<sup>366</sup> Hence, it is clear that such control of internal communication in DNA systems paves the way for rational design of DNA-based Turing patterns in closed systems.

## 6. Conclusions

Autonomous biological materials are mesmerizing. It is unlikely that any synthetic materials will approach the complexity, robustness and adaptability of biological ones soon. Solutions evolved over millions of years can however stimulate imagination and inspire the development of exciting new autonomous, active and adaptive molecular systems, materials and functional devices. By aiming for an understanding of the concepts and molecular mechanisms driving each function, one also realizes that common motives are spanning under the apparent complexity.

This also applies to synthetic systems, where the feedback mechanisms driving inorganic, enzymatic and DNA-based

out-of-equilibrium systems are surprisingly similar. Different out-of-equilibrium functions such as temporal control, work-generation or adaptive behavior, can be implemented in diverse molecular systems *via* non-linear chemical reaction networks, often assisted by enzymes or catalysts. Compartmentalization, immobilization and control of the diffusion speed of reactants and catalysts are emerging as tools to gain deeper control over feedback mechanisms extending beyond the possibilities of homogeneous bulk solutions.

On the conceptual side, the rational implementation of out-of-equilibrium functions with DNA based systems often clarifies the relation between mechanisms and functions – most complex behavior can be realized, but DNA faces some ultimate challenges in terms of scalable applications into materials.

When developing a new out-of-equilibrium system it is important to clearly identify the energy source (fuel), the processing unit (catalyst), and the feedback controls (autocatalyst, activator and inhibitor). In an ideal case the fuel provides the energy, the catalytic unit drives the function, and feedback mechanisms regulate the characteristic timescale and interactions of the out-of-equilibrium system. A clear identification of these units should also promote the development of modular systems where multiple catalytic units that consume compatible or orthogonal fuels communicate and drive function in a cooperative fashion.

While there has been success in the direction of logic operations, computational algorithms, sensing and communication, some of the more unsolved fundamental challenges refer to concepts of self-replicating, self-evolving, and even learning systems. Towards real-life applications, it is of course desirable to foster the integration of established and emerging concepts into materials. Adaptive and autonomous devices, and sensors are certainly one key aspect, while implants and biomaterials that can actively adapt and interact with the body provide other great opportunities for complex molecular systems.

## Acknowledgements

We acknowledge support from the DFG (WA 3084/4-1) and the European Research Council (TimeProSAMat) ERC grant agreement no. 677960.

## References

- 1 N. N. Taleb, *The black swan: the impact of the highly improbable*, Random House, New York, 2007.
- 2 E. Mattia and S. Otto, *Nat. Nanotechnol.*, 2015, **10**, 111–119.
- 3 I. R. Epstein and B. Xu, *Nat. Nanotechnol.*, 2016, **11**, 312–319.
- 4 L. Heinen and A. Walther, *Soft Matter*, 2015, **11**, 7857–7866.
- 5 H. W. H. van Roekel, B. J. H. M. Rosier, L. H. H. Meijer, P. A. J. Hilbers, A. J. Markvoort, W. T. S. Huck and T. F. A. de Greef, *Chem. Soc. Rev.*, 2015, **44**, 7465–7483.
- 6 S. C. Warren, O. Guney-Albay and B. A. Grzybowski, *J. Phys. Chem. Lett.*, 2012, **3**, 2103–2111.
- 7 M. C. Cross and P. C. Hohenberg, *Rev. Mod. Phys.*, 1993, **65**, 851–1112.

- 8 S. Mann, *Angew. Chem., Int. Ed.*, 2008, **47**, 5306–5320.
- 9 Y. Tu, F. Peng, A. Adawy, Y. Men, L. K. E. A. Abdelmohsen and D. A. Wilson, *Chem. Rev.*, 2015, **116**, 2023–2078.
- 10 B. Novák and J. J. Tyson, *Nat. Rev. Mol. Cell Biol.*, 2008, **9**, 981–991.
- 11 T. Y. C. Tsai, Y. S. Choi, W. Z. Ma, J. R. Pomerening, C. Tang and J. E. Ferrell, *Science*, 2008, **321**, 126–129.
- 12 C. H. Ko and J. S. Takahashi, *Hum. Mol. Genet.*, 2006, **15**, R271–R277.
- 13 M. Gallego and D. M. Virshup, *Nat. Rev. Mol. Cell Biol.*, 2007, **8**, 139–148.
- 14 F. Guillaumond, H. Dardente, V. Giguere and N. Cermakian, *J. Biol. Rhythms*, 2005, **20**, 391–403.
- 15 J. A. Mohawk, C. B. Green and J. S. Takahashi, *Annu. Rev. Neurosci.*, 2012, **35**, 445–462.
- 16 S. H. Yoo, S. Yamazaki, P. L. Lowrey, K. Shimomura, C. H. Ko, E. D. Buhr, S. M. Siepka, H. K. Hong, W. J. Oh, O. J. Yoo, M. Menaker and J. S. Takahashi, *Proc. Natl. Acad. Sci. U. S. A.*, 2004, **101**, 5339–5346.
- 17 S. M. Reppert and D. R. Weaver, *Nature*, 2002, **418**, 935–941.
- 18 B. P. Bean, *Nat. Rev. Neurosci.*, 2007, **8**, 451–465.
- 19 A. L. Hodgkin and A. F. Huxley, *J. Physiol.*, 1952, **117**, 500–544.
- 20 R. B. Robinson, *Annu. Rev. Physiol.*, 2003, **65**, 453–480.
- 21 B. P. Belousov, *Sb. Ref. Radiats. Med.*, 1958, **147**, 145.
- 22 A. N. Zaikin and A. M. Zhabotinsky, *Nature*, 1970, **225**, 535–537.
- 23 R. J. Field, R. M. Noyes and E. Koros, *J. Am. Chem. Soc.*, 1972, **94**, 8649–8664.
- 24 W. C. Bray, *J. Am. Chem. Soc.*, 1921, **43**, 1262–1267.
- 25 T. S. Briggs and W. C. Rauscher, *J. Chem. Educ.*, 1973, **50**, 496.
- 26 I. R. Epstein, *J. Chem. Educ.*, 1989, **66**, 191.
- 27 M. Orbán, P. Dekepper, I. R. Epstein and K. Kustin, *Nature*, 1981, **292**, 816–818.
- 28 G. Rábai, M. T. Beck, K. Kustin and I. R. Epstein, *J. Phys. Chem.*, 1989, **93**, 2853–2858.
- 29 M. Orbán, P. De Kepper and I. R. Epstein, *J. Am. Chem. Soc.*, 1982, **104**, 2657–2658.
- 30 G. Rábai, K. Kustin and I. R. Epstein, *J. Am. Chem. Soc.*, 1989, **111**, 3870–3874.
- 31 I. R. Epstein and K. Showalter, *J. Phys. Chem.*, 1996, **100**, 13132–13147.
- 32 I. R. Epstein, *An Introduction to Nonlinear Chemical Dynamics: Oscillations, Waves, Patterns, and Chaos*, Oxford University Press, USA, 1998.
- 33 M. A. C. Stuart, W. T. S. Huck, J. Genzer, M. Müller, C. Ober, M. Stamm, G. B. Sukhorukov, I. Szleifer, V. V. Tsukruk, M. Urban, F. Winnik, S. Zauscher, I. Luzinov and S. Minko, *Nat. Mater.*, 2010, **9**, 101–113.
- 34 M. Orbán, K. Kurin-Csörgei and I. R. Epstein, *Acc. Chem. Res.*, 2015, **48**, 593–601.
- 35 M. Orbán and I. R. Epstein, *J. Am. Chem. Soc.*, 1985, **107**, 2302–2305.
- 36 Y. Luo and I. R. Epstein, *J. Am. Chem. Soc.*, 1991, **113**, 1518–1522.
- 37 G. A. Frerichs, T. M. Mlnarik, R. J. Grun and R. C. Thompson, *J. Phys. Chem. A*, 2001, **105**, 829–837.
- 38 E. Poros, V. Horváth, K. Kurin-Csörgei, I. R. Epstein and M. Orbán, *J. Am. Chem. Soc.*, 2011, **133**, 7174–7179.
- 39 L. Kuhnert, K. I. Agladze and V. I. Krinsky, *Nature*, 1989, **337**, 244–247.
- 40 K. J. M. Bishop and B. A. Grzybowski, *Phys. Rev. Lett.*, 2006, **97**, 128702.
- 41 R. Yoshida, T. Takahashi, T. Yamaguchi and H. Ichijo, *J. Am. Chem. Soc.*, 1996, **118**, 5134–5135.
- 42 K. Kovacs, R. E. McIlwaine, S. K. Scott and A. F. Taylor, *J. Phys. Chem. A*, 2007, **111**, 549–551.
- 43 A. Goldbeter and S. R. Caplan, *Annu. Rev. Biophys.*, 1976, **5**, 449–476.
- 44 S. R. Caplan, A. Naparstek and N. J. Zabusky, *Nature*, 1973, **245**, 364–366.
- 45 A. Naparstek, D. Thomas and S. R. Caplan, *Biochim. Biophys. Acta*, 1973, **323**, 643–646.
- 46 C. G. Hocker, I. R. Epstein, K. Kustin and K. Tornheim, *Biophys. Chem.*, 1994, **51**, 21–35.
- 47 V. K. Vanag, D. G. Míguez and I. R. Epstein, *J. Chem. Phys.*, 2006, **125**, 194515.
- 48 G. Hu, J. A. Pojman, S. K. Scott, M. M. Wrobel and A. F. Taylor, *J. Phys. Chem. B*, 2010, **114**, 14059–14063.
- 49 T. Heuser, E. Weyandt and A. Walther, *Angew. Chem., Int. Ed.*, 2015, **54**, 13258–13262.
- 50 S. N. Semenov, A. S. Y. Wong, R. M. van der Made, S. G. J. Postma, J. Groen, H. W. H. van Roekel, T. F. A. de Greef and W. T. S. Huck, *Nat. Chem.*, 2015, **7**, 160–165.
- 51 A. S. Y. Wong, S. G. J. Postma, I. N. Vialshin, S. N. Semenov and W. T. S. Huck, *J. Am. Chem. Soc.*, 2015, **137**, 12415–12420.
- 52 M. B. Elowitz and S. Leibler, *Nature*, 2000, **403**, 335–338.
- 53 J. Stricker, S. Cookson, M. R. Bennett, W. H. Mather, L. S. Tsimring and J. Hasty, *Nature*, 2008, **456**, 516–519.
- 54 V. Noireaux, R. Bar-ziv and A. Libchaber, *Proc. Natl. Acad. Sci. U. S. A.*, 2003, **100**, 12672–12677.
- 55 J. Shin and V. Noireaux, *ACS Synth. Biol.*, 2012, **1**, 29–41.
- 56 E. Karzbrun, A. M. Tayar, V. Noireaux and R. H. Bar-Ziv, *Science*, 2014, **345**, 829–832.
- 57 K. Montagne, R. Plisson, Y. Sakai, T. Fujii and Y. Rondelez, *Mol. Syst. Biol.*, 2011, **7**, 466.
- 58 J. Kim and E. Winfree, *Mol. Syst. Biol.*, 2011, **7**, 465.
- 59 T. Fujii and Y. Rondelez, *ACS Nano*, 2013, **7**, 27–34.
- 60 A. Baccouche, K. Montagne, A. Padirac, T. Fujii and Y. Rondelez, *Methods*, 2014, **67**, 234–249.
- 61 D. Y. Zhang and G. Seelig, *Nat. Chem.*, 2011, **3**, 103–113.
- 62 D. Soloveichik, G. Seelig and E. Winfree, *Proc. Natl. Acad. Sci. U. S. A.*, 2010, **107**, 5393–5398.
- 63 D. Y. Zhang and E. Winfree, *J. Am. Chem. Soc.*, 2009, **131**, 17303–17314.
- 64 R. R. F. Machinek, T. E. Ouldridge, N. E. C. Haley, J. Bath and A. J. Turberfield, *Nat. Commun.*, 2014, **5**, 5324.
- 65 G. Seelig, B. Yurke and E. Winfree, *J. Am. Chem. Soc.*, 2006, **128**, 12211–12220.
- 66 G. Seelig, D. Soloveichik, D. Y. Zhang and E. Winfree, *Science*, 2006, **314**, 1585–1588.
- 67 D. Y. Zhang, A. J. Turberfield, B. Yurke and E. Winfree, *Science*, 2007, **318**, 1121–1125.

- 68 D. A. Fletcher and D. Mullins, *Nature*, 2010, **463**, 485–492.
- 69 T. Mitchison and M. Kirschner, *Nature*, 1984, **312**, 237–242.
- 70 I. M. Cheeseman and A. Desai, *Nat. Rev. Mol. Cell Biol.*, 2008, **9**, 33–46.
- 71 A. Desai and T. J. Mitchison, *Annu. Rev. Cell Dev. Biol.*, 1997, **13**, 83–117.
- 72 M. Caudron, G. Bunt, P. Bastiaens and E. Karsenti, *Science*, 2005, **309**, 1373–1376.
- 73 A. Akhmanova and M. O. Steinmetz, *Nat. Rev. Mol. Cell Biol.*, 2008, **9**, 309–322.
- 74 T. D. Pollard, *Annu. Rev. Biophys. Biomol. Struct.*, 2007, **36**, 451–477.
- 75 T. D. Pollard and J. A. Cooper, *Science*, 2009, **326**, 1208–1212.
- 76 P. K. Mattila and P. Lappalainen, *Nat. Rev. Mol. Cell Biol.*, 2008, **9**, 446–454.
- 77 E. D. Korn, *Physiol. Rev.*, 1982, **62**, 672–737.
- 78 P. K. Kundu, D. Samanta, R. Leizrowice, B. Margulis, H. Zhao, M. Börner, T. Udayabhaskararao, D. Manna and R. Klajn, *Nat. Chem.*, 2015, **7**, 646–652.
- 79 R. Klajn, P. J. Wesson, K. J. M. Bishop and B. A. Grzybowski, *Angew. Chem., Int. Ed.*, 2009, **48**, 7035–7039.
- 80 A. R. Hirst, S. Roy, M. Arora, A. K. Das, N. Hodson, P. Murray, S. Marshall, N. Javid, J. Sefcik, J. Boekhoven, J. H. van Esch, S. Santabarbara, N. T. Hunt and R. V. Ulijn, *Nat. Chem.*, 2010, **2**, 1089–1094.
- 81 J. Boekhoven, J. M. Poolman, C. Maity, F. Li, L. van der Mee, C. B. Minkeberg, E. Mendes, J. H. van Esch and R. Eelkema, *Nat. Chem.*, 2013, **5**, 433–437.
- 82 J. M. A. Carnall, C. A. Waudby, A. M. Belenguer, M. C. A. Stuart, J. J. P. Peyralans and S. Otto, *Science*, 2010, **327**, 1502–1506.
- 83 M. Colomb-Delsuc, E. Mattia, J. W. Sadownik and S. Otto, *Nat. Commun.*, 2015, **6**, 7427.
- 84 A. Pal, M. Malakoutikhah, G. Leonetti, M. Tezcan, M. Colomb-Delsuc, V. D. Nguyen, J. van der Gucht and S. Otto, *Angew. Chem., Int. Ed.*, 2015, **54**, 7852–7856.
- 85 W. L. Noorduin, A. Grinthal, L. Mahadevan and J. Aizenberg, *Science*, 2013, **340**, 832–837.
- 86 R. Klajn, M. Fialkowski, I. T. Bensemann, A. Bitner, C. J. Campbell, K. Bishop, S. Smoukov and B. A. Grzybowski, *Nat. Mater.*, 2004, **3**, 729–735.
- 87 J. Boekhoven, M. Koot, T. A. Wezendonk, R. Eelkema and E. J. H. van, *J. Am. Chem. Soc.*, 2012, **134**, 12908–12911.
- 88 J. S. Mohammed and W. L. Murphy, *Adv. Mater.*, 2009, **21**, 2361–2374.
- 89 J. M. Hu, G. Q. Zhang and S. Y. Liu, *Chem. Soc. Rev.*, 2012, **41**, 5933–5949.
- 90 A. Alouane, R. Labruère, T. Le Saux, F. Schmidt and L. Jullien, *Angew. Chem., Int. Ed.*, 2015, **54**, 7492–7509.
- 91 B. A. Grzybowski, H. A. Stone and G. M. Whitesides, *Nature*, 2000, **405**, 1033–1036.
- 92 B. A. Grzybowski and G. M. Whitesides, *Science*, 2002, **296**, 718–721.
- 93 M. Irie, *J. Am. Chem. Soc.*, 1983, **105**, 2078–2079.
- 94 H. J. Liu, Y. Xu, F. Y. Li, Y. Yang, W. X. Wang, Y. L. Song and D. S. Liu, *Angew. Chem., Int. Ed.*, 2007, **46**, 2515–2517.
- 95 Y. Jiang, P. Wan, H. Xu, Z. Wang, X. Zhang and M. Smet, *Langmuir*, 2009, **25**, 10134–10138.
- 96 S. Silvi, A. Arduini, A. Pochini, A. Secchi, M. Tomasulo, F. M. Raymo, M. Baroncini and A. Credi, *J. Am. Chem. Soc.*, 2007, **129**, 13378–13379.
- 97 M. Emond, T. Le Saux, J. F. Allemand, P. Pelupessy, R. Plasson and L. Jullien, *Chem. – Eur. J.*, 2012, **18**, 14375–14383.
- 98 D. L. Thomsen, P. Keller, J. Naciri, R. Pink, H. Jeon, D. Shenoy and B. R. Ratna, *Macromolecules*, 2001, **34**, 5868–5875.
- 99 S. Iamsaard, S. J. Asshoff, B. Matt, T. Kudernac, J. Cornelissen, S. P. Fletcher and N. Katsonis, *Nat. Chem.*, 2014, **6**, 229–235.
- 100 X. K. Liu and M. Jiang, *Angew. Chem., Int. Ed.*, 2006, **45**, 3846–3850.
- 101 A. Manna, P. L. Chen, H. Akiyama, T. X. Wei, K. Tamada and W. Knoll, *Chem. Mater.*, 2003, **15**, 20–28.
- 102 A. A. Beharry, O. Sadovski and G. A. Woolley, *J. Am. Chem. Soc.*, 2011, **133**, 19684–19687.
- 103 R. Klajn, K. J. M. Bishop and B. A. Grzybowski, *Proc. Natl. Acad. Sci. U. S. A.*, 2007, **104**, 10305–10309.
- 104 D. Manna, T. Udayabhaskararao, H. Zhao and R. Klajn, *Angew. Chem., Int. Ed.*, 2015, **54**, 12394–12397.
- 105 H. Zhao, S. Sen, T. Udayabhaskararao, M. Sawczyk, K. Kucanda, D. Manna, P. K. Kundu, J. W. Lee, P. Kral and R. Klajn, *Nat. Nanotechnol.*, 2016, **11**, 82–88.
- 106 T. Heuser, A.-K. Steppert, C. Molano Lopez, B. Zhu and A. Walther, *Nano Lett.*, 2015, **15**, 2213–2219.
- 107 C. Pezzato and L. J. Prins, *Nat. Commun.*, 2015, **6**, 7790.
- 108 S. Maiti, I. Fortunati, C. Ferrante, P. Scrimin and L. J. Prins, *Nat. Chem.*, 2016, **8**, 725–731.
- 109 S. Debnath, S. Roy and R. V. Ulijn, *J. Am. Chem. Soc.*, 2013, **135**, 16789–16792.
- 110 C. G. Pappas, I. R. Sasselli and R. V. Ulijn, *Angew. Chem., Int. Ed.*, 2015, **54**, 8119–8123.
- 111 J. Boekhoven, A. M. Brizard, K. N. K. Kowlgi, G. J. M. Koper, R. Eelkema and J. H. van Esch, *Angew. Chem., Int. Ed.*, 2010, **49**, 4825–4828.
- 112 J. Boekhoven, W. E. Hendriksen, G. J. M. Koper, R. Eelkema and J. H. van Esch, *Science*, 2015, **349**, 1075–1079.
- 113 R. Yoshida, T. Sakai, S. Ito and T. Yamaguchi, *J. Am. Chem. Soc.*, 2002, **124**, 8095–8098.
- 114 T. Ueki, M. Shibayama and R. Yoshida, *Chem. Commun.*, 2013, **49**, 6947–6949.
- 115 D. Suzuki, T. Sakai and R. Yoshida, *Angew. Chem., Int. Ed.*, 2008, **47**, 917–920.
- 116 D. Suzuki, H. Taniguchi and R. Yoshida, *J. Am. Chem. Soc.*, 2009, **131**, 12058–12059.
- 117 R. Yoshida, H. Ichijo, T. Hakuta and T. Yamaguchi, *Macromol. Rapid Commun.*, 1995, **16**, 305–310.
- 118 C. J. Crook, A. Smith, R. A. L. Jones and A. J. Ryan, *Phys. Chem. Chem. Phys.*, 2002, **4**, 1367–1369.
- 119 I. Varga, I. Szalai, R. Mészáros and T. Gilányi, *J. Phys. Chem. B*, 2006, **110**, 20297–20301.
- 120 I. Lagzi, B. Kowalczyk, D. Wang and B. A. Grzybowski, *Angew. Chem., Int. Ed.*, 2010, **49**, 8616–8619.
- 121 I. Lagzi, D. Wang, B. Kowalczyk and B. A. Grzybowski, *Langmuir*, 2010, **26**, 13770–13772.

- 122 T. Liedl and F. C. Simmel, *Nano Lett.*, 2005, **5**, 1894–1898.
- 123 T. Liedl, M. Olapinski and F. C. Simmel, *Angew. Chem., Int. Ed.*, 2006, **45**, 5007–5010.
- 124 X.-J. Qi, C.-H. Lu, X. Liu, S. Shimron, H.-H. Yang and I. Willner, *Nano Lett.*, 2013, **13**, 4920–4924.
- 125 J. Horváth, I. Szalai, J. Boissonade and P. De Kepper, *Soft Matter*, 2011, **7**, 8462–8472.
- 126 V. Labrot, P. De Kepper, J. Boissonade, I. Szalai and F. Gauffre, *J. Phys. Chem. B*, 2005, **109**, 21476–21480.
- 127 X. He, M. Aizenberg, O. Kuksenok, L. D. Zarzar, A. Shastri, A. C. Balazs and J. Aizenberg, *Nature*, 2012, **487**, 214–218.
- 128 E. Franco, E. Friedrichs, J. Kim, R. Jungmann, R. Murray, E. Winfree and F. C. Simmel, *Proc. Natl. Acad. Sci. U. S. A.*, 2011, **108**, E784–E793.
- 129 J. H. Marden and L. R. Allen, *Proc. Natl. Acad. Sci. U. S. A.*, 2002, **99**, 4161–4166.
- 130 A. Coskun, M. Banaszak, R. D. Astumian, J. F. Stoddart and B. A. Grzybowski, *Chem. Soc. Rev.*, 2012, **41**, 19–30.
- 131 N. Hirokawa and Y. Noda, *Physiol. Rev.*, 2008, **88**, 1089–1118.
- 132 A. Gennerich and R. D. Vale, *Curr. Opin. Cell Biol.*, 2009, **21**, 59–67.
- 133 R. D. Vale and R. A. Milligan, *Science*, 2000, **288**, 88–95.
- 134 M. J. Schnitzer and S. M. Block, *Nature*, 1997, **388**, 386–390.
- 135 M. Schliwa and G. Woehlke, *Nature*, 2003, **422**, 759–765.
- 136 E. P. Sablin, R. B. Case, S. C. Dai, C. L. Hart, A. Ruby, R. D. Vale and R. J. Fletterick, *Nature*, 1998, **395**, 813–816.
- 137 E. M. Purcell, *Am. J. Phys.*, 1977, **45**, 3–11.
- 138 H. C. Berg, *Annu. Rev. Biochem.*, 2003, **72**, 19–54.
- 139 M. Yoshida, E. Muneyuki and T. Hisabori, *Nat. Rev. Mol. Cell Biol.*, 2001, **2**, 669–677.
- 140 P. D. Boyer, *Annu. Rev. Biochem.*, 1997, **66**, 717–749.
- 141 T. P. Loisel, R. Boujemaa, D. Pantaloni and M. F. Carlier, *Nature*, 1999, **401**, 613–616.
- 142 M. D. Welch, A. Iwamatsu and T. J. Mitchison, *Nature*, 1997, **385**, 265–269.
- 143 F. Frischknecht, V. Moreau, S. Röttger, S. Gonfloni, I. Reckmann, G. Superti-Furga and M. Way, *Nature*, 1999, **401**, 926–929.
- 144 J. M. Squire, *Curr. Opin. Struct. Biol.*, 1997, **7**, 247–257.
- 145 H. L. Sweeney and A. Houdusse, *Annu. Rev. Biophys.*, 2010, **39**, 539–557.
- 146 R. S. Adelstein and E. Eisenberg, *Annu. Rev. Biochem.*, 1980, **49**, 921–956.
- 147 R. K. Soong, G. D. Bachand, H. P. Neves, A. G. Olkhovets, H. G. Craighead and C. D. Montemagno, *Science*, 2000, **290**, 1555–1558.
- 148 K. J. Böhm, R. Stracke, P. Mühlig and E. Unger, *Nanotechnology*, 2001, **12**, 238–244.
- 149 H. Hess, J. Clemmens, D. Qin, J. Howard and V. Vogel, *Nano Lett.*, 2001, **1**, 235–239.
- 150 O. J. N. Bertrand, D. K. Fygenson and O. A. Saleh, *Proc. Natl. Acad. Sci. U. S. A.*, 2012, **109**, 17342–17347.
- 151 A. J. M. Wollman, C. Sanchez-Cano, H. M. J. Carstairs, R. A. Cross and A. J. Turberfield, *Nat. Nanotechnol.*, 2014, **9**, 44–47.
- 152 H. Hess, *Annu. Rev. Biomed. Eng.*, 2011, **13**, 429–450.
- 153 E. R. Kay, D. A. Leigh and F. Zerbetto, *Angew. Chem., Int. Ed.*, 2007, **46**, 72–191.
- 154 S. Erbas-Cakmak, D. A. Leigh, C. T. McTernan and A. L. Nussbaumer, *Chem. Rev.*, 2015, **115**, 10081–10206.
- 155 P. L. Anelli, N. Spencer and J. F. Stoddart, *J. Am. Chem. Soc.*, 1991, **113**, 5131–5133.
- 156 D. A. Leigh, J. K. Y. Wong, F. Dehez and F. Zerbetto, *Nature*, 2003, **424**, 174–179.
- 157 S. P. Fletcher, F. Dumur, M. M. Pollard and B. L. Feringa, *Science*, 2005, **310**, 80–82.
- 158 C. Cheng, P. R. McGonigal, S. T. Schniebeli, H. Li, N. A. Vermeulen, C. Ke and J. F. Stoddart, *Nat. Nanotechnol.*, 2015, **10**, 547–553.
- 159 N. Koumura, R. W. J. Zijlstra, R. A. van Delden, N. Harada and B. L. Feringa, *Nature*, 1999, **401**, 152–155.
- 160 N. Koumura, E. M. Geertsema, A. Meetsma and B. L. Feringa, *J. Am. Chem. Soc.*, 2000, **122**, 12005–12006.
- 161 M. Klok, N. Boyle, M. T. Pryce, A. Meetsma, W. R. Browne and B. L. Feringa, *J. Am. Chem. Soc.*, 2008, **130**, 10484–10485.
- 162 M. K. J. ter Wiel, R. A. van Delden, A. Meetsma and B. L. Feringa, *J. Am. Chem. Soc.*, 2003, **125**, 15076–15086.
- 163 N. Ruangsupapichat, M. M. Pollard, S. R. Harutyunyan and B. L. Feringa, *Nat. Chem.*, 2011, **3**, 53–60.
- 164 J. Chen, J. C. M. Kistemaker, J. Robertus and B. L. Feringa, *J. Am. Chem. Soc.*, 2014, **136**, 14924–14932.
- 165 G. Ragazzon, M. Baroncini, S. Silvi, M. Venturi and A. Credi, *Nat. Nanotechnol.*, 2015, **10**, 70–75.
- 166 T. Kudernac, N. Ruangsupapichat, M. Parschau, B. Macía, N. Katsonis, S. R. Harutyunyan, K. H. Ernst and B. L. Feringa, *Nature*, 2011, **479**, 208–211.
- 167 M. von Delius and D. A. Leigh, *Chem. Soc. Rev.*, 2011, **40**, 3656–3676.
- 168 M. von Delius, E. M. Geertsema and D. A. Leigh, *Nat. Chem.*, 2010, **2**, 96–101.
- 169 J. S. Shin and N. A. Pierce, *J. Am. Chem. Soc.*, 2004, **126**, 10834–10835.
- 170 W. B. Sherman and N. C. Seeman, *Nano Lett.*, 2004, **4**, 1203–1207.
- 171 P. Yin, H. Yan, X. G. Daniell, A. J. Turberfield and J. H. Reif, *Angew. Chem., Int. Ed.*, 2004, **43**, 4906–4911.
- 172 Y. Chen, M. Wang and C. Mao, *Angew. Chem., Int. Ed.*, 2004, **43**, 3554–3557.
- 173 Y. Tian, Y. He, Y. Chen, P. Yin and C. D. Mao, *Angew. Chem., Int. Ed.*, 2005, **44**, 4355–4358.
- 174 J. Bath, S. J. Green and A. J. Turberfield, *Angew. Chem., Int. Ed.*, 2005, **44**, 4358–4361.
- 175 K. Lund, A. J. Manzo, N. Dabby, N. Michelotti, A. Johnson-Buck, J. Nangreave, S. Taylor, R. Pei, M. N. Stojanovic, N. G. Walter, E. Winfree and H. Yan, *Nature*, 2010, **465**, 206–210.
- 176 T.-G. Cha, J. Pan, H. Chen, J. Salgado, X. Li, C. Mao and J. H. Choi, *Nat. Nanotechnol.*, 2014, **9**, 39–43.
- 177 S. F. J. Wickham, M. Endo, Y. Katsuda, K. Hidaka, J. Bath, H. Sugiyama and A. J. Turberfield, *Nat. Nanotechnol.*, 2011, **6**, 166–169.
- 178 K. Yehl, A. Mugler, S. Vivek, Y. Liu, Y. Zhang, M. Fan, E. R. Weeks and K. Salaita, *Nat. Nanotechnol.*, 2016, **11**, 184–190.

- 179 P. Yin, H. M. T. Choi, C. R. Calvert and N. A. Pierce, *Nature*, 2008, **451**, 318–322.
- 180 R. A. Muscat, J. Bath and A. J. Turberfield, *Nano Lett.*, 2011, **11**, 982–987.
- 181 R. A. Muscat, J. Bath and A. J. Turberfield, *Small*, 2012, **8**, 3593–3597.
- 182 S. F. J. Wickham, J. Bath, Y. Katsuda, M. Endo, K. Hidaka, H. Sugiyama and A. J. Turberfield, *Nat. Nanotechnol.*, 2012, **7**, 169–173.
- 183 T. Omabegho, R. Sha and N. C. Seeman, *Science*, 2009, **324**, 67–71.
- 184 S. J. Green, J. Bath and A. J. Turberfield, *Phys. Rev. Lett.*, 2008, **101**, 238101.
- 185 J. Bath, S. J. Green, K. E. Allen and A. J. Turberfield, *Small*, 2009, **5**, 1513–1516.
- 186 R. Dreyfus, J. Baudry, M. L. Roper, M. Fermigier, H. A. Stone and J. Bibette, *Nature*, 2005, **437**, 862–865.
- 187 C. Tomlinson, *Proc. R. Soc. London*, 1860, **11**, 575–577.
- 188 M. Nagayama, S. Nakata, Y. Doi and Y. Hayashima, *Physica D*, 2004, **194**, 151–165.
- 189 S. Nakata, J. Kirisaka, Y. Arima and T. Ishii, *J. Phys. Chem. B*, 2006, **110**, 21131–21134.
- 190 S. Nakata and M. Murakami, *Langmuir*, 2010, **26**, 2414–2417.
- 191 Y. Ikezoe, G. Washino, T. Uemura, S. Kitagawa and H. Matsui, *Nat. Mater.*, 2012, **11**, 1081–1085.
- 192 W. Gao, A. Pei and J. Wang, *ACS Nano*, 2012, **6**, 8432–8438.
- 193 F. Mou, C. Chen, H. Ma, Y. Yin, Q. Wu and J. Guan, *Angew. Chem., Int. Ed.*, 2013, **52**, 7208–7212.
- 194 W. Gao, A. Uygun and J. Wang, *J. Am. Chem. Soc.*, 2012, **134**, 897–900.
- 195 S. Venkataraman, R. M. Dirks, P. W. K. Rothmund, E. Winfree and N. A. Pierce, *Nat. Nanotechnol.*, 2007, **2**, 490–494.
- 196 R. A. Pavlick, S. Sengupta, T. McFadden, H. Zhang and A. Sen, *Angew. Chem., Int. Ed.*, 2011, **50**, 9374–9377.
- 197 J. Leckie, A. Hope, M. Hughes, S. Debnath, S. Fleming, A. W. Wark, R. V. Ulijn and M. D. Haw, *ACS Nano*, 2014, **8**, 9580–9589.
- 198 R. F. Ismagilov, A. Schwartz, N. Bowden and G. M. Whitesides, *Angew. Chem., Int. Ed.*, 2002, **41**, 652–654.
- 199 W. F. Paxton, K. C. Kistler, C. C. Olmeda, A. Sen, S. K. St. Angelo, Y. Cao, T. E. Mallouk, P. E. Lammert and V. H. Crespi, *J. Am. Chem. Soc.*, 2004, **126**, 13424–13431.
- 200 T. R. Kline, W. F. Paxton, T. E. Mallouk and A. Sen, *Angew. Chem., Int. Ed.*, 2005, **44**, 744–746.
- 201 Y. Wang, R. M. Hernandez, D. J. Bartlett, J. M. Bingham, T. R. Kline, A. Sen and T. E. Mallouk, *Langmuir*, 2006, **22**, 10451–10456.
- 202 J. R. Howse, R. A. L. Jones, A. J. Ryan, T. Gough, R. Vafabakhsh and R. Golestanian, *Phys. Rev. Lett.*, 2007, **99**, 048102.
- 203 T.-C. Lee, M. Alarcón-Correa, C. Miksch, K. Hahn, J. G. Gibbs and P. Fischer, *Nano Lett.*, 2014, **14**, 2407–2412.
- 204 L. Baraban, D. Makarov, R. Streubel, I. Mönch, D. Grimm, S. Sanchez and O. G. Schmidt, *ACS Nano*, 2012, **6**, 3383–3389.
- 205 Y. Wu, Z. Wu, X. Lin, Q. He and J. Li, *ACS Nano*, 2012, **6**, 10910–10916.
- 206 A. A. Solovev, Y. Mei, E. Bermúdez Ureña, G. Huang and O. G. Schmidt, *Small*, 2009, **5**, 1688–1692.
- 207 W. Gao, S. Sattayasamitsathit, J. Orozeo and J. Wang, *J. Am. Chem. Soc.*, 2011, **133**, 11862–11864.
- 208 D. A. Wilson, R. J. M. Nolte and J. C. M. van Hest, *Nat. Chem.*, 2012, **4**, 268–274.
- 209 S. Sanchez, L. Soler and J. Katuri, *Angew. Chem., Int. Ed.*, 2015, **54**, 1414–1444.
- 210 N. Mano and A. Heller, *J. Am. Chem. Soc.*, 2005, **127**, 11574–11575.
- 211 I.-A. Pavel, A.-I. Bunea, S. David and S. Gáspár, *Chem. CatChem*, 2014, **6**, 866–872.
- 212 S. Sanchez, A. A. Solovev, Y. F. Mei and O. G. Schmidt, *J. Am. Chem. Soc.*, 2010, **132**, 13144–13145.
- 213 D. Pantarotto, W. R. Browne and B. L. Feringa, *Chem. Commun.*, 2008, 1533–1535.
- 214 K. K. Dey, X. Zhao, B. M. Tansi, W. J. Méndez-Ortiz, U. M. Córdova-Figueroa, R. Golestanian and A. Sen, *Nano Lett.*, 2015, **15**, 8311–8315.
- 215 X. Ma, A. Jannasch, U.-R. Albrecht, K. Hahn, A. Miguel-López, E. Schäffer and S. Sánchez, *Nano Lett.*, 2015, **15**, 7043–7050.
- 216 H. S. Muddana, S. Sengupta, T. E. Mallouk, A. Sen and P. J. Butler, *J. Am. Chem. Soc.*, 2010, **132**, 2110–2111.
- 217 S. Sengupta, K. K. Dey, H. S. Muddana, T. Tabouillot, M. E. Ibele, P. J. Butler and A. Sen, *J. Am. Chem. Soc.*, 2013, **135**, 1406–1414.
- 218 S. Sengupta, M. M. Spiering, K. K. Dey, W. T. Duan, D. Patra, P. J. Butler, R. D. Astumian, S. J. Benkovic and A. Sen, *ACS Nano*, 2014, **8**, 2410–2418.
- 219 H. Yu, K. Jo, K. L. Kounovsky, J. J. de Pablo and D. C. Schwartz, *J. Am. Chem. Soc.*, 2009, **131**, 5722–5723.
- 220 S. Sahu, T. H. LaBean and J. H. Reif, *Nano Lett.*, 2008, **8**, 3870–3878.
- 221 C. Riedel, R. Gabizon, C. A. M. Wilson, K. Hamadani, K. Tsekouras, S. Marqusee, S. Pressé and C. Bustamante, *Nature*, 2015, **517**, 227–230.
- 222 R. Golestanian, *Phys. Rev. Lett.*, 2015, **115**, 108102.
- 223 L. Ionov, *Mater. Today*, 2014, **17**, 494–503.
- 224 K. Ichimura, S. K. Oh and M. Nakagawa, *Science*, 2000, **288**, 1624–1626.
- 225 A. E. Aliev, J. Y. Oh, M. E. Kozlov, A. A. Kuznetsov, S. L. Fang, A. F. Fonseca, R. Ovalle, M. D. Lima, M. H. Haque, Y. N. Gartstein, M. Zhang, A. A. Zakhidov and R. H. Baughman, *Science*, 2009, **323**, 1575–1578.
- 226 M. Morimoto and M. Irie, *J. Am. Chem. Soc.*, 2010, **132**, 14172–14178.
- 227 S. Kobatake, S. Takami, H. Muto, T. Ishikawa and M. Irie, *Nature*, 2007, **446**, 778–781.
- 228 Y. Yu, M. Nakano and T. Ikeda, *Nature*, 2003, **425**, 145.
- 229 T. Ikeda, M. Nakano, Y. L. Yu, O. Tsutsumi and A. Kanazawa, *Adv. Mater.*, 2003, **15**, 201–205.
- 230 A. Natansohn and P. Rochon, *Chem. Rev.*, 2002, **102**, 4139–4176.
- 231 H. F. Yu and T. Ikeda, *Adv. Mater.*, 2011, **23**, 2149–2180.

- 232 M. Yamada, M. Kondo, R. Miyasato, Y. Naka, J. Mamiya, M. Kinoshita, A. Shishido, Y. L. Yu, C. J. Barrett and T. Ikeda, *J. Mater. Chem.*, 2009, **19**, 60–62.
- 233 M. Camacho-Lopez, H. Finkelmann, P. Palffy-Muhoray and M. Shelley, *Nat. Mater.*, 2004, **3**, 307–310.
- 234 C. L. van Oosten, C. W. M. Bastiaansen and D. J. Broer, *Nat. Mater.*, 2009, **8**, 677–682.
- 235 M. Yamada, M. Kondo, J.-i. Mamiya, Y. Yu, M. Kinoshita, C. J. Barrett and T. Ikeda, *Angew. Chem., Int. Ed.*, 2008, **47**, 4986–4988.
- 236 T. Hugel, N. B. Holland, A. Cattani, L. Moroder, M. Seitz and H. E. Gaub, *Science*, 2002, **296**, 1103–1106.
- 237 G. Du, E. Moulin, N. Jouault, E. Buhler and N. Giuseppone, *Angew. Chem., Int. Ed.*, 2012, **51**, 12504–12508.
- 238 R. Eelkema, M. M. Pollard, J. Vicario, N. Katsonis, B. S. Ramon, C. W. M. Bastiaansen, D. J. Broer and B. L. Feringa, *Nature*, 2006, **440**, 163.
- 239 Q. Li, G. Fuks, E. Moulin, M. Maaloum, M. Rawiso, I. Kulic, J. T. Foy and N. Giuseppone, *Nat. Nanotechnol.*, 2015, **10**, 161–165.
- 240 A. Goujon, G. Du, E. Moulin, G. Fuks, M. Maaloum, E. Buhler and N. Giuseppone, *Angew. Chem., Int. Ed.*, 2016, **55**, 703–707.
- 241 J. R. Howse, P. Topham, C. J. Crook, A. J. Gleeson, W. Bras, R. A. L. Jones and A. J. Ryan, *Nano Lett.*, 2006, **6**, 73–77.
- 242 P. D. Topham, J. R. Howse, C. J. Crook, S. P. Armes, R. A. L. Jones and A. J. Ryan, *Macromolecules*, 2007, **40**, 4393–4395.
- 243 Y. Shiraki and R. Yoshida, *Angew. Chem., Int. Ed.*, 2012, **51**, 6112–6116.
- 244 Y. Murase, S. Maeda, S. Hashimoto and R. Yoshida, *Langmuir*, 2009, **25**, 483–489.
- 245 R. Yoshida, M. Tanaka, S. Onodera, T. Yamaguchi and E. Kokufuta, *J. Phys. Chem. A*, 2000, **104**, 7549–7555.
- 246 V. V. Yashin and A. C. Balazs, *Science*, 2006, **314**, 798–801.
- 247 V. V. Yashin, O. Kuksenok, P. Dayal and A. C. Balazs, *Rep. Prog. Phys.*, 2012, **75**, 066601.
- 248 Y. Takeoka, M. Watanabe and R. Yoshida, *J. Am. Chem. Soc.*, 2003, **125**, 13320–13321.
- 249 S. Maeda, Y. Hara, R. Yoshida and S. Hashimoto, *Angew. Chem., Int. Ed.*, 2008, **47**, 6690–6693.
- 250 R. Yoshida and Y. Murase, *Colloids Surf., B*, 2012, **99**, 60–66.
- 251 Y. Shiraki, A. M. Akimoto, T. Miyata and R. Yoshida, *Chem. Mater.*, 2014, **26**, 5441–5443.
- 252 O. Tabata, H. Hirasawa, S. Aoki, R. Yoshida and E. Kokufuta, *Sens. Actuators, A*, 2002, **95**, 234–238.
- 253 S. Maeda, Y. Hara, T. Sakai, R. Yoshida and S. Hashimoto, *Adv. Mater.*, 2007, **19**, 3480–3484.
- 254 O. Kuksenok, V. V. Yashin, M. Kinoshita, T. Sakai, R. Yoshida and A. C. Balazs, *J. Mater. Chem.*, 2011, **21**, 8360–8371.
- 255 D. Suzuki, T. Kobayashi, R. Yoshida and T. Hirai, *Soft Matter*, 2012, **8**, 11447–11449.
- 256 R. Mitsunaga, K. Okeyoshi and R. Yoshida, *Chem. Commun.*, 2013, **49**, 4935–4937.
- 257 Y. Zhang, N. Zhou, N. Li, M. G. Sun, D. Kim, S. Fraden, I. R. Epstein and B. Xu, *J. Am. Chem. Soc.*, 2014, **136**, 7341–7347.
- 258 G. H. Wadhams and J. P. Armitage, *Nat. Rev. Mol. Cell Biol.*, 2004, **5**, 1024–1037.
- 259 S. L. Porter, G. H. Wadhams and J. P. Armitage, *Nat. Rev. Microbiol.*, 2011, **9**, 153–165.
- 260 Y. A. Xiong, C. H. Huang, P. A. Iglesias and P. N. Devreotes, *Proc. Natl. Acad. Sci. U. S. A.*, 2010, **107**, 17079–17086.
- 261 K. F. Swaney, C.-H. Huang and P. N. Devreotes, *Annu. Rev. Biophys.*, 2010, **39**, 265–289.
- 262 P. A. Iglesias and P. N. Devreotes, *Curr. Opin. Cell Biol.*, 2012, **24**, 245–253.
- 263 P. J. M. Van Haastert and P. N. Devreotes, *Nat. Rev. Mol. Cell Biol.*, 2004, **5**, 626–634.
- 264 E. G. Ruby, *Annu. Rev. Microbiol.*, 1996, **50**, 591–624.
- 265 W.-L. Ng and B. L. Bassler, *Annu. Rev. Genet.*, 2009, **43**, 197–222.
- 266 C. M. Waters and B. L. Bassler, *Annu. Rev. Cell Dev. Biol.*, 2005, **21**, 319–346.
- 267 B. S. Goldman, W. C. Nierman, D. Kaiser, S. C. Slater, A. S. Durkin, J. A. Eisen, C. M. Ronning, W. B. Barbazuk, M. Blanchard, C. Field, C. Halling, G. Hinkle, O. Iartchuk, H. S. Kim, C. Mackenzie, R. Madupu, N. Miller, A. Shvartsbeyn, S. A. Sullivan, M. Vaudin, R. Wiegand and H. B. Kaplan, *Proc. Natl. Acad. Sci. U. S. A.*, 2006, **103**, 15200–15205.
- 268 B. L. Bassler and R. Losick, *Cell*, 2006, **125**, 237–246.
- 269 D. Kaiser, *Annu. Rev. Microbiol.*, 2004, **58**, 75–98.
- 270 T. Nakagaki, H. Yamada and A. Tóth, *Nature*, 2000, **407**, 470.
- 271 A. Tero, S. Takagi, T. Saigusa, K. Ito, D. P. Bebbert, M. D. Fricker, K. Yumiki, R. Kobayashi and T. Nakagaki, *Science*, 2010, **327**, 439–442.
- 272 A. M. Turing, *Philos. Trans. R. Soc. London, Ser. B*, 1952, **237**, 37–72.
- 273 S. Kondo and T. Miura, *Science*, 2010, **329**, 1616–1620.
- 274 S. Kondo and R. Asai, *Nature*, 1995, **376**, 765–768.
- 275 Y. Hong, N. M. K. Blackman, N. D. Kopp, A. Sen and D. Velegol, *Phys. Rev. Lett.*, 2007, **99**, 178103.
- 276 F. Peng, Y. Tu, J. C. M. van Hest and D. A. Wilson, *Angew. Chem., Int. Ed.*, 2015, **54**, 11662–11665.
- 277 K. K. Dey, S. Das, M. F. Poyton, S. Sengupta, P. J. Butler, P. S. Cremer and A. Sen, *ACS Nano*, 2014, **8**, 11941–11949.
- 278 J. Wang and W. Gao, *ACS Nano*, 2012, **6**, 5745–5751.
- 279 J. Burdick, R. Laocharoensuk, P. M. Wheat, J. D. Posner and J. Wang, *J. Am. Chem. Soc.*, 2008, **130**, 8164–8165.
- 280 Y. Wu, X. Lin, Z. Wu, H. Moehwald and Q. He, *ACS Appl. Mater. Interfaces*, 2014, **6**, 10476–10481.
- 281 K. K. Dey, S. Bhandari, D. Bandyopadhyay, S. Basu and A. Chattopadhyay, *Small*, 2013, **9**, 1916–1920.
- 282 Y. Ikezoe, J. Fang, T. L. Wasik, M. Shi, T. Uemura, S. Kitagawa and H. Matsui, *Nano Lett.*, 2015, **15**, 4019–4023.
- 283 I. Lagzi, S. Soh, P. J. Wesson, K. P. Browne and B. A. Grzybowski, *J. Am. Chem. Soc.*, 2010, **132**, 1198–1199.
- 284 J. Orozco, V. Garcia-Gradilla, M. D'Agostino, W. Gao, A. Cortés and J. Wang, *ACS Nano*, 2013, **7**, 818–824.
- 285 Z. Wu, X. Lin, Y. Wu, T. Si, J. Sun and Q. He, *ACS Nano*, 2014, **8**, 6097–6105.

- 286 X. Lu, L. Ren, Q. Gao, Y. Zhao, S. Wang, J. Yang and I. R. Epstein, *Chem. Commun.*, 2013, **49**, 7690–7692.
- 287 S. Shinohara, T. Seki, T. Sakai, R. Yoshida and Y. Takeoka, *Angew. Chem., Int. Ed.*, 2008, **47**, 9039–9043.
- 288 S. Shinohara, T. Seki, T. Sakai, R. Yoshida and Y. Takeoka, *Chem. Commun.*, 2008, 4735–4737.
- 289 P. Dayal, O. Kuksenok and A. C. Balazs, *Langmuir*, 2009, **25**, 4298–4301.
- 290 P. Dayal, O. Kuksenok and A. C. Balazs, *Soft Matter*, 2010, **6**, 768–773.
- 291 Y. Benenson, *Nat. Rev. Genet.*, 2012, **13**, 455–468.
- 292 A. Aviram, *J. Am. Chem. Soc.*, 1988, **110**, 5687–5692.
- 293 A. P. de Silva and S. Uchiyama, *Nat. Nanotechnol.*, 2007, **2**, 399–410.
- 294 J. Andréasson and U. Pischel, *Chem. Soc. Rev.*, 2015, **44**, 1053–1069.
- 295 E. Katz and V. Privman, *Chem. Soc. Rev.*, 2010, **39**, 1835–1857.
- 296 E. Katz, *Curr. Opin. Biotechnol.*, 2015, **34**, 202–208.
- 297 C. C. Wu, S. Wan, W. J. Hou, L. Q. Zhang, J. H. Xu, C. Cui, Y. Y. Wang, J. Hu and W. H. Tan, *Chem. Commun.*, 2015, **51**, 3723–3734.
- 298 R. Orbach, B. Willner and I. Willner, *Chem. Commun.*, 2015, **51**, 4144–4160.
- 299 T. Niazov, R. Baron, E. Katz, O. Lioubashevski and I. Willner, *Proc. Natl. Acad. Sci. U. S. A.*, 2006, **103**, 17160–17163.
- 300 R. Baron, O. Lioubashevski, E. Katz, T. Niazov and I. Willner, *J. Phys. Chem. A*, 2006, **110**, 8548–8553.
- 301 L. Amir, T. K. Tam, M. Pita, M. M. Meijler, L. Alfonta and E. Katz, *J. Am. Chem. Soc.*, 2009, **131**, 826–832.
- 302 I. Tokarev, V. Gopishetty, J. Zhou, M. Pita, M. Motornov, E. Katz and S. Minko, *ACS Appl. Mater. Interfaces*, 2009, **1**, 532–536.
- 303 M. Motornov, J. Zhou, M. Pita, V. Gopishetty, I. Tokarev, E. Katz and S. Minko, *Nano Lett.*, 2008, **8**, 2993–2997.
- 304 M. Ikeda, T. Tanida, T. Yoshii, K. Kurotani, S. Onogi, K. Urayama and I. Hamachi, *Nat. Chem.*, 2014, **6**, 511–518.
- 305 M. N. Stojanovic, T. E. Mitchell and D. Stefanovic, *J. Am. Chem. Soc.*, 2002, **124**, 3555–3561.
- 306 J. Elbaz, F. A. Wang, F. Remacle and I. Willner, *Nano Lett.*, 2012, **12**, 6049–6054.
- 307 M. Moshe, J. Elbaz and I. Willner, *Nano Lett.*, 2009, **9**, 1196–1200.
- 308 F. Wang, R. Orbach and I. Willner, *Chem. – Eur. J.*, 2012, **18**, 16030–16036.
- 309 B. Shlyahovsky, Y. Li, O. Lioubashevski, J. Elbaz and I. Willner, *ACS Nano*, 2009, **3**, 1831–1843.
- 310 R. Orbach, F. Wang, O. Lioubashevski, R. D. Levine, F. Remacle and I. Willner, *Chem. Sci.*, 2014, **5**, 3381–3387.
- 311 J. Elbaz, O. Lioubashevski, F. A. Wang, F. Remacle, R. D. Levine and I. Willner, *Nat. Nanotechnol.*, 2010, **5**, 417–422.
- 312 S. M. Douglas, I. Bachelet and G. M. Church, *Science*, 2012, **335**, 831–834.
- 313 R. Baron, O. Lioubashevski, E. Katz, T. Niazov and I. Willner, *Angew. Chem., Int. Ed.*, 2006, **45**, 1572–1576.
- 314 G. Strack, M. Ornatska, M. Pita and E. Katz, *J. Am. Chem. Soc.*, 2008, **130**, 4234–4235.
- 315 H. Lederman, J. Macdonald, D. Stefanovic and M. N. Stojanovic, *Biochemistry*, 2006, **45**, 1194–1199.
- 316 M. N. Stojanovic and D. Stefanovic, *J. Am. Chem. Soc.*, 2003, **125**, 6673–6676.
- 317 M. N. Stojanovic and D. Stefanovic, *Nat. Biotechnol.*, 2003, **21**, 1069–1074.
- 318 J. Macdonald, Y. Li, M. Sutovic, H. Lederman, K. Pendri, W. Lu, B. L. Andrews, D. Stefanovic and M. N. Stojanovic, *Nano Lett.*, 2006, **6**, 2598–2603.
- 319 C. W. Brown, M. R. Lakin, E. K. Horwitz, M. L. Fanning, H. E. West, D. Stefanovic and S. W. Graves, *Angew. Chem., Int. Ed.*, 2014, **53**, 7183–7187.
- 320 R. J. Pei, E. Matamoros, M. H. Liu, D. Stefanovic and M. N. Stojanovic, *Nat. Nanotechnol.*, 2010, **5**, 773–777.
- 321 L. Qian and E. Winfree, *J. R. Soc., Interface*, 2011, **8**, 1281–1297.
- 322 X. Chen, N. Briggs, J. R. McLain and A. D. Ellington, *Proc. Natl. Acad. Sci. U. S. A.*, 2013, **110**, 5386–5391.
- 323 L. Qian and E. Winfree, *Science*, 2011, **332**, 1196–1201.
- 324 Y. J. Chen, N. Dalchau, N. Srinivas, A. Phillips, L. Cardelli, D. Soloveichik and G. Seelig, *Nat. Nanotechnol.*, 2013, **8**, 755–762.
- 325 L. Qian, E. Winfree and J. Bruck, *Nature*, 2011, **475**, 368–372.
- 326 A. J. Genot, T. Fujii and Y. Rondelez, *Phys. Rev. Lett.*, 2012, **109**, 208102.
- 327 A. Padirac, T. Fujii and Y. Rondelez, *Proc. Natl. Acad. Sci. U. S. A.*, 2012, **109**, E3212–E3220.
- 328 J. Kim, K. S. White and E. Winfree, *Mol. Syst. Biol.*, 2006, **2**, 68.
- 329 A. J. Genot, T. Fujii and Y. Rondelez, *J. R. Soc., Interface*, 2013, **10**, 20130212.
- 330 D. Kagan, S. Balasubramanian and J. Wang, *Angew. Chem., Int. Ed.*, 2011, **50**, 503–506.
- 331 W. Gao, A. Pei, R. Dong and J. Wang, *J. Am. Chem. Soc.*, 2014, **136**, 2276–2279.
- 332 M. Ibele, T. E. Mallouk and A. Sen, *Angew. Chem., Int. Ed.*, 2009, **48**, 3308–3312.
- 333 W. Duan, R. Liu and A. Sen, *J. Am. Chem. Soc.*, 2013, **135**, 1280–1283.
- 334 S. Saha, R. Golestanian and S. Ramaswamy, *Phys. Rev. E*, 2014, **89**, 062316.
- 335 J. Palacci, S. Sacanna, A. P. Steinberg, D. J. Pine and P. M. Chaikin, *Science*, 2013, **339**, 936–940.
- 336 M. E. Ibele, P. E. Lammert, V. H. Crespi and A. Sen, *ACS Nano*, 2010, **4**, 4845–4851.
- 337 A. F. Taylor, M. R. Tinsley, F. Wang, Z. Huang and K. Showalter, *Science*, 2009, **323**, 614–617.
- 338 A. F. Taylor, G. R. Armstrong, N. Goodchild and S. K. Scott, *Phys. Chem. Chem. Phys.*, 2003, **5**, 3928–3932.
- 339 S. Tateyama, Y. Shibuta and R. Yoshida, *J. Phys. Chem. B*, 2008, **112**, 1777–1782.
- 340 M. Toiya, H. O. González-Ochoa, V. K. Vanag, S. Fraden and I. R. Epstein, *J. Phys. Chem. Lett.*, 2010, **1**, 1241–1246.
- 341 V. V. Yashin, S. Suzuki, R. Yoshida and A. C. Balazs, *J. Mater. Chem.*, 2012, **22**, 13625–13636.
- 342 G. V. Kolmakov, V. V. Yashin, S. P. Levitan and A. C. Balazs, *Proc. Natl. Acad. Sci. U. S. A.*, 2010, **107**, 12417–12422.

- 343 P. Dayal, O. Kuksenok, A. Bhattacharya and A. C. Balazs, *J. Mater. Chem.*, 2012, **22**, 241–250.
- 344 P. Dayal, O. Kuksenok and A. C. Balazs, *Proc. Natl. Acad. Sci. U. S. A.*, 2013, **110**, 431–436.
- 345 O. Kuksenok, P. Dayal, A. Bhattacharya, V. V. Yashin, D. Deb, I. C. Chen, K. J. Van Vliet and A. C. Balazs, *Chem. Soc. Rev.*, 2013, **42**, 7257–7277.
- 346 M. M. Wrobel, T. Bánsági Jr, S. K. Scott, A. F. Taylor, C. O. Bounds, A. Carranza and J. A. Pojman, *Biophys. J.*, 2012, **103**, 610–615.
- 347 D. G. Míguez, V. K. Vanag and I. R. Epstein, *Proc. Natl. Acad. Sci. U. S. A.*, 2007, **104**, 6992–6997.
- 348 S. N. Semenov, A. J. Markvoort, T. F. A. de Greef and W. T. S. Huck, *Angew. Chem., Int. Ed.*, 2014, **53**, 8066–8069.
- 349 S. M. Chirieleison, P. B. Allen, Z. B. Simpson, A. D. Ellington and X. Chen, *Nat. Chem.*, 2013, **5**, 1000–1005.
- 350 J. Horváth, I. Szalai and P. De Kepper, *Science*, 2009, **324**, 772–775.
- 351 T. Bánsági, V. K. Vanag and I. R. Epstein, *Science*, 2011, **331**, 1309–1312.
- 352 S. N. Semenov, A. J. Markvoort, W. B. L. Gevers, A. Piruska, T. F. A. de Greef and W. T. S. Huck, *Biophys. J.*, 2013, **105**, 1057–1066.
- 353 A. T. Winfree, *Science*, 1972, **175**, 634–636.
- 354 K. I. Agladze and V. I. Krinsky, *Nature*, 1982, **296**, 424–426.
- 355 S. C. Müller, T. Plessner and B. Hess, *Science*, 1985, **230**, 661–663.
- 356 V. Perez-Muñozuri, R. Aliev, B. Vasiev, V. Perez-Villar and V. I. Krinsky, *Nature*, 1991, **353**, 740–742.
- 357 L. Kuhnert, *Nature*, 1986, **319**, 393–394.
- 358 I. R. Epstein, V. K. Vanag, A. C. Balazs, O. Kuksenok, P. Dayal and A. Bhattacharya, *Acc. Chem. Res.*, 2012, **45**, 2160–2168.
- 359 A. Kaminaga, V. K. Vanag and I. R. Epstein, *Angew. Chem., Int. Ed.*, 2006, **45**, 3087–3089.
- 360 V. K. Vanag and I. R. Epstein, *Proc. Natl. Acad. Sci. U. S. A.*, 2003, **100**, 14635–14638.
- 361 V. K. Vanag and I. R. Epstein, *Science*, 2001, **294**, 835–837.
- 362 V. K. Vanag and I. R. Epstein, *Phys. Rev. Lett.*, 2001, **87**, 228301.
- 363 V. K. Vanag and I. R. Epstein, *Chaos*, 2008, **18**, 026107.
- 364 V. Castets, E. Dulos, J. Boissonade and P. De Kepper, *Phys. Rev. Lett.*, 1990, **64**, 2953–2956.
- 365 A. Padirac, T. Fujii, A. Estévez-Torres and Y. Rondelez, *J. Am. Chem. Soc.*, 2013, **135**, 14586–14592.
- 366 A. S. Zadorin, Y. Rondelez, J.-C. Galas and A. Estevez-Torres, *Phys. Rev. Lett.*, 2015, **114**, 068301.